First principle calculations of thermodynamic parameters and phase equilibrium

Igor A. Abrikosov

Theoretical Physics,

Department of Physics, Chemistry and Biology, Linköping University, Sweden

igor.abrikosov@ifm.liu.se

Contents:

- Phase stability: general consideration and phenomenological approaches.
- Empirical models (Miedema's empirical model for enthalpies of formation, Pettifor structural map, Hume-Rothery rules).
- Calculations of phase diagrams. Thermodynamic approach.
- From thermodynamics towards statistical mechanics.
- The cluster expansion method
- The Monte-Carlo method
- The global structure optimization problem

Steel vs cast iron

Iron with up to 2% carbon is a base material for steels.

Steel 60Si2

Tempered steel annealed at 700oC

Electron microscopy x12000.

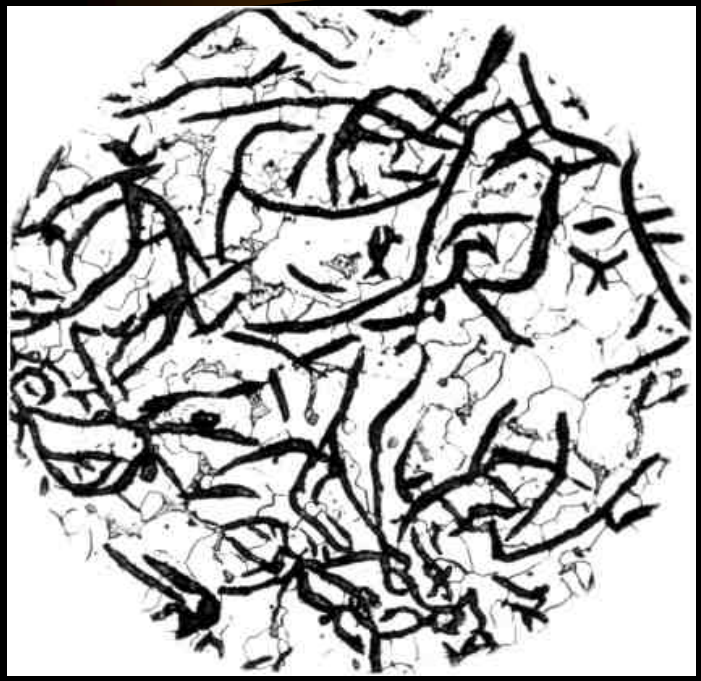

More than 2.06 % carbon in Fe leads to a formation of cast iron

Nanocomposite hard coating (Ti-Al)N alloys

- The new universal high-performance coating (drilling, milling, etc.)
- Increasing Al content leads to very high heat resistance, dry high-speed machining, and increased oxidation resistance
- Spinodal decomposition

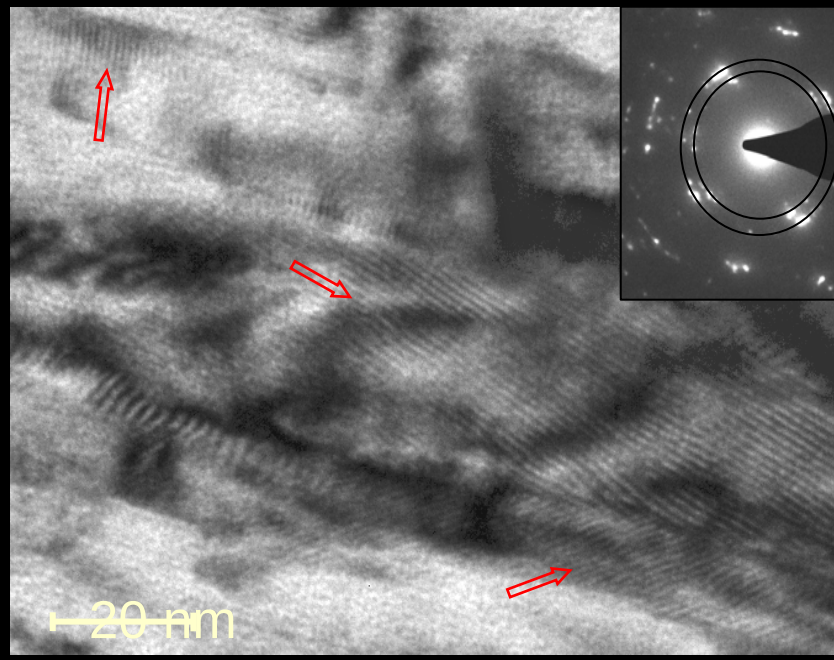

Multiscale modeling

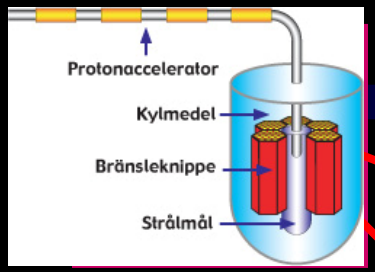

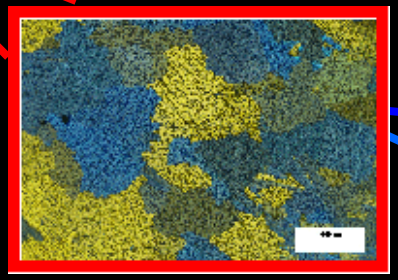

Microstructure
- Grains
≅ 1 – 10 mm
Properties
• High cycle fatigue
• Ductility

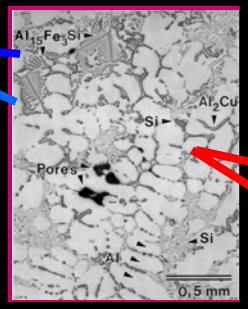

Microstructure
- Phases
≅ 100 – 500 microns
Properties
• Yield strength
• Ultimate tensile strength
• High cycle fatigue
• Low cycle fatigue
• **Thermal Growth**
• Ductility

Microstructure
- Phases
≅ 3-100 nanometers
Properties
• Yield strength
• Ultimate tensile strength
• Low cycle fatigue
• Ductility

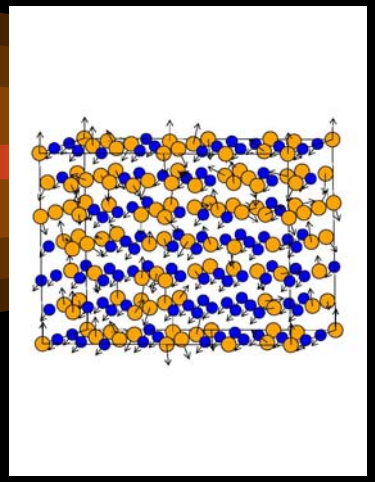

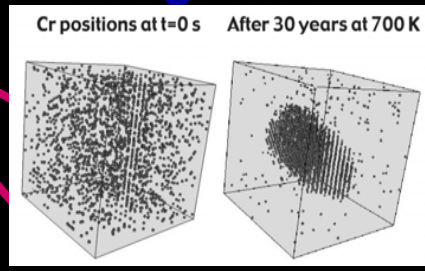

Atoms
≅ 10-100 Angstroms
Properties
• Thermal Growth

Original idea for this figure belongs to Chris Wolverton Ford Motor Company

GOAL:

The main aim of this lecture is not so much to present the existing results of first-principles calculations of phase equilibria in alloys or to describe the available software for statistical simulations, but to give a more general view of the problem and to describe the used techniques with a primary concern of their validity and accuracy.

We will learn the theory behind the simulations!

Phase diagrams

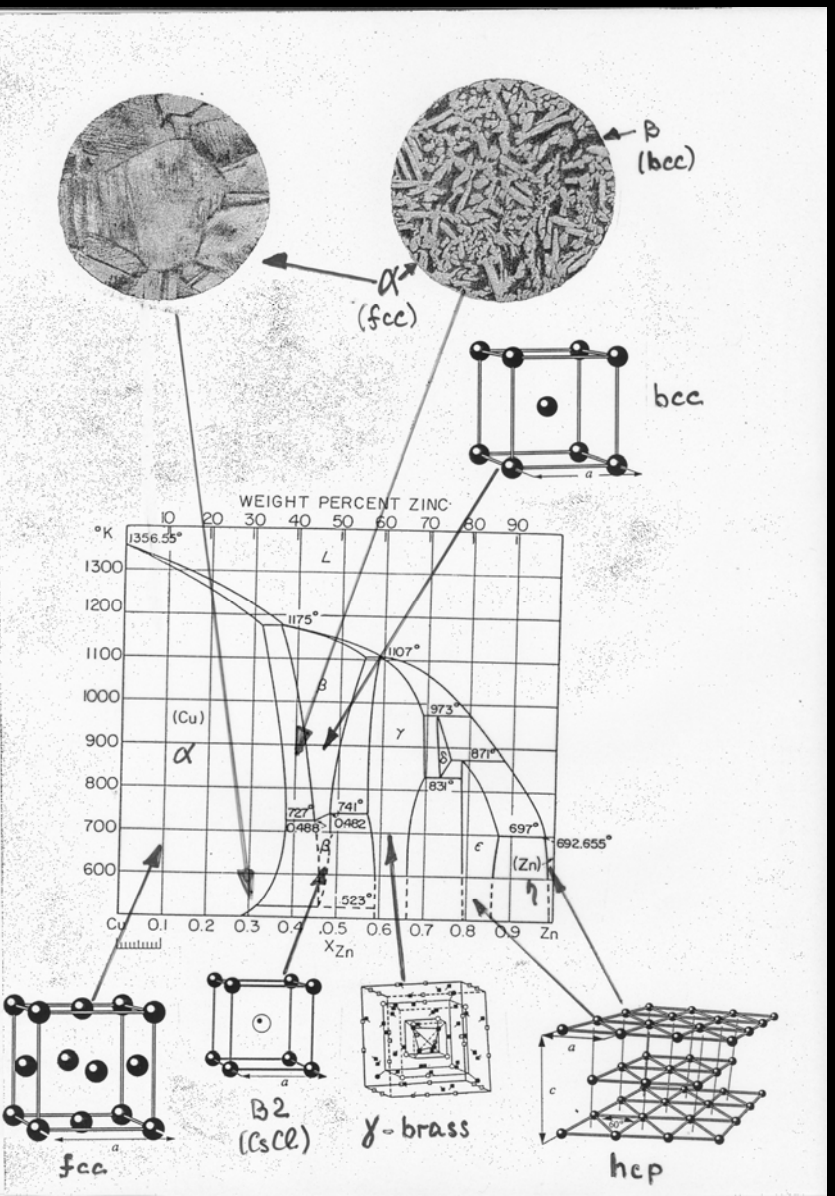

- A phase is defined as a homogeneous region of matter, separated from other homogeneous regions by phase boundaries.
- The different phases will have different physical and/or chemical properties.
- Phase diagram is a graphical representation of the loci of thermodynamic variables when equilibrium among the phases of a system is established under a given set of conditions, like temperature, pressure, composition, and size scale.
- Departures from equilibrium will occur in any real system.

Hume-Rothery rules (from T. B. Massalski, "Structure of solid solutions")

- 15% rule. If difference between the atomic sizes of the component elements forming an alloy exceeds 15%, solid solubility should become restricted
- The electrochemical effect. Formation of stable intermediate compounds will restrict primary solid solubility.
- The relative valence effect. The extent of solid solubility and the stability of certain intermediate phases is determined by the electron concentration.

The second Hume-Rothery rule

$$c_0(T) \sim \exp[-Q_X/(k_B T)]$$

$$Q_X = E_X^{imp} - \frac{k}{k+m} E_{A_k X_m}^{form}$$

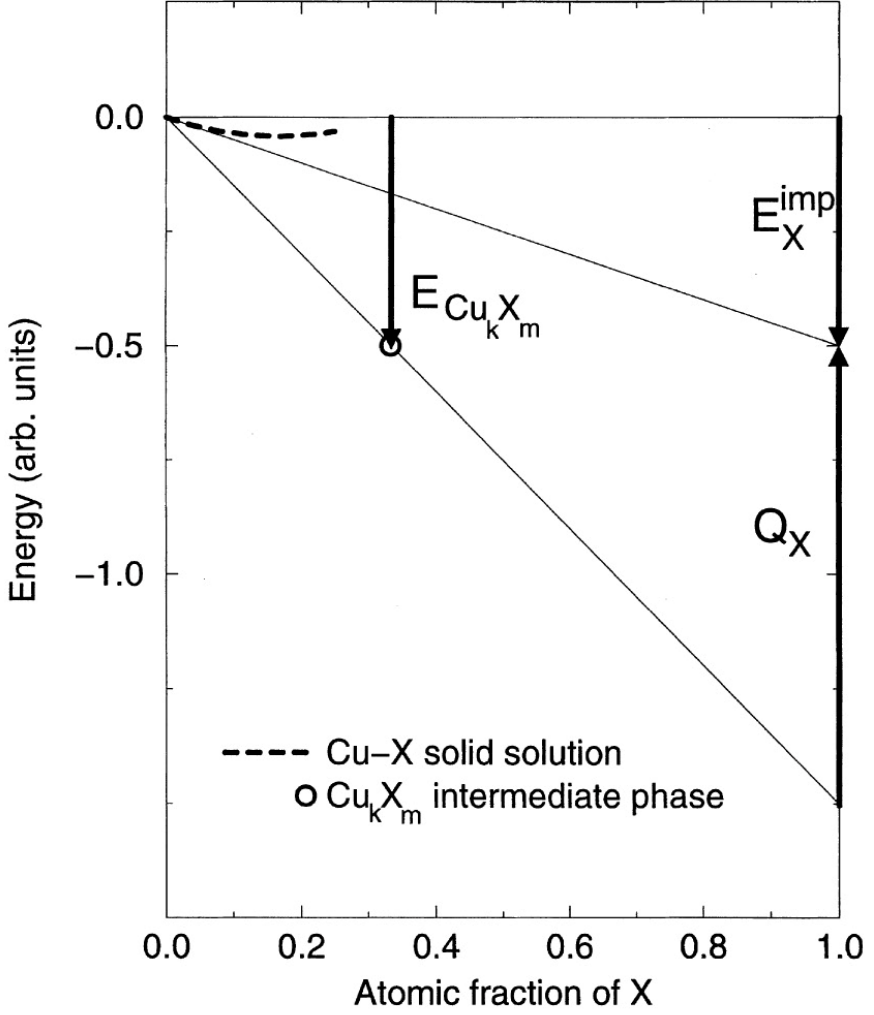

Fig. 2. Schematic representation of the phase equilibrium between Cu–X solid solution and a stoichiometric Cu_kX_m intermediate phase. Mixing energy of the solid solution as a function of the solute concentration is shown by a dashed line. The formation energy of the Cu_kX_m phase ($E^{f}_{Cu_kX_m}$), the impurity solution energy (E^{imp}_{X}), and the energy of the dissolution reaction (Q_X) are indicated by arrows. The lengths and the directions of the arrows represent the absolute values and the signs, respectively, of the corresponding quantities.

Phase diagrams for Cu-Zn and Ag-Zn

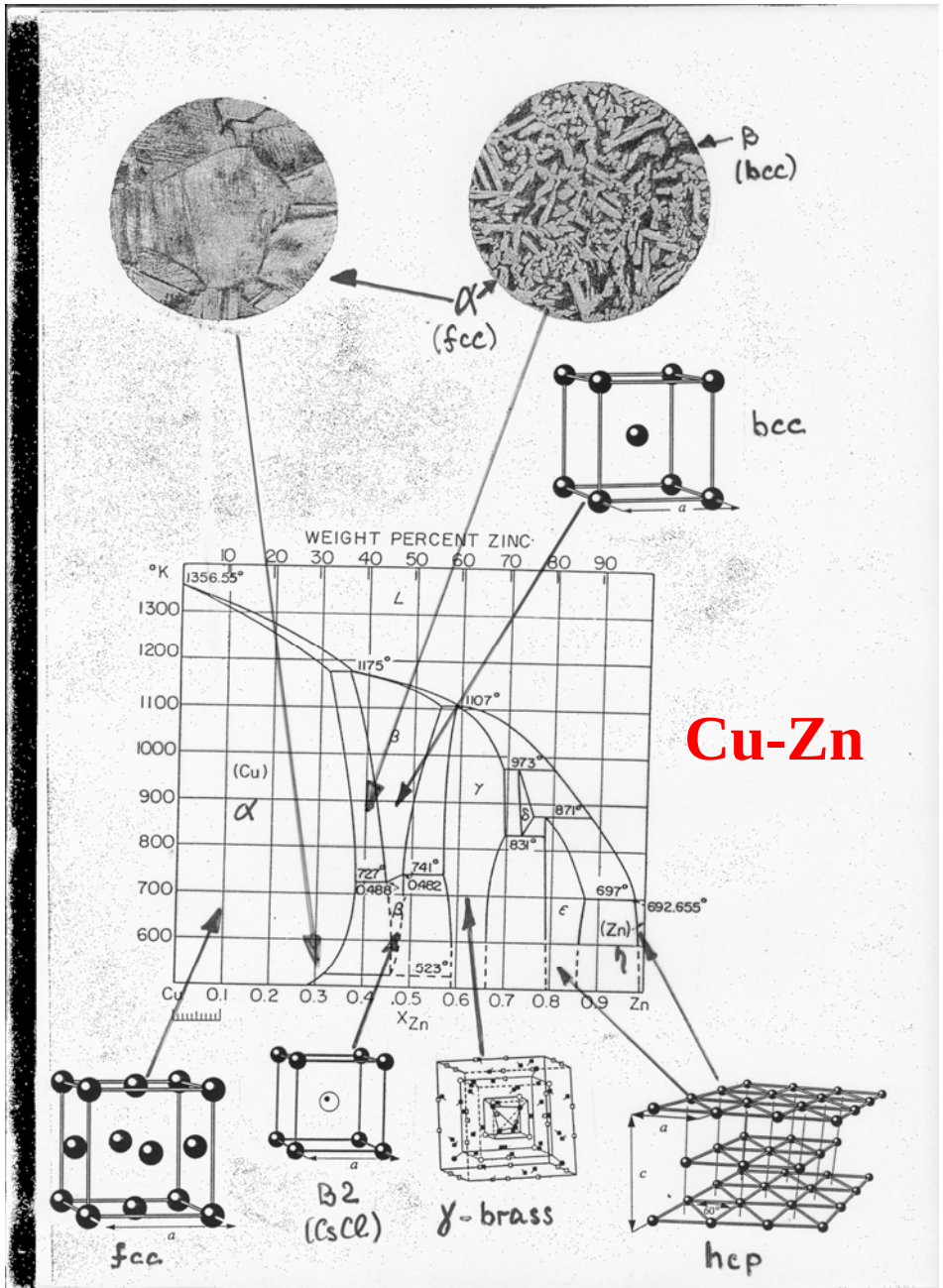

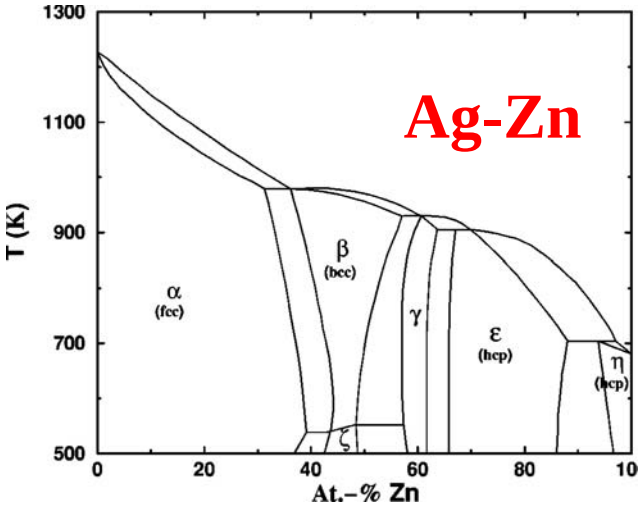

Miedema's model of alloy formation: $\Delta H = E^{alloy} - c E^{A} - (1-c) E^{B}$

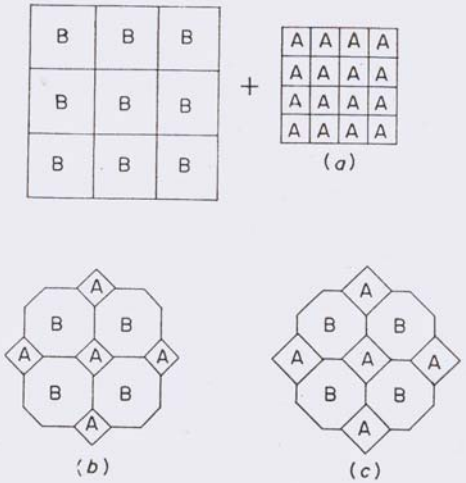

Fig. 4 Formation of an alloy in the 'macroscopic atom' model. In a first step atomic cells are taken from the metals to form the alloy with just a small change in shape but not in volume. In a second step, and owing to the change in boundary conditions, the atomic volumes change slightly. This change in boundary conditions is responsible for the heat of formation of the alloy. Redrawn after Miedema and de Châtel.[37]

(+) : Charge redistribution at the cell boundary $\sim \Delta n_b^{2/3}$

(−) : Charge transfer in order to equalize the chemical potential in the alloy $\sim (\Delta\Phi)^2$

$$\Delta H = f(c)\left[-P(\Delta\Phi)^2 + Q(\Delta n_b^{1/3})^2\right]$$

For solid solutions one additionally includes an elastic energy contribution (size mismatch) and structure dependent enthalpy (structure mismatch).

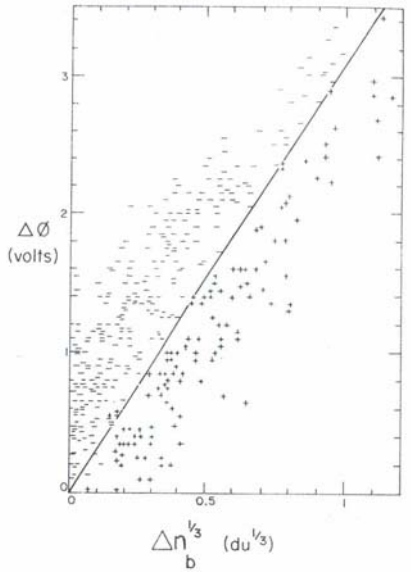

Fig. 10 Test of (3.3) for the sign of the heat of formation of alloys, in solid binary systems in which one metal is a transition or noble metal and the other a transition, noble, alkaline or alkaline-earth metal. Each binary system is characterized by its values of $\Delta\phi$ and $\Delta n_b^{1/3}$. − indicates that the binary system contains stable intermetallic compounds, which implies that ΔH is negative. + indicates that the binary system contains no compound and in addition there is limited solid solubility (< 10 at. % at both sides); this indicates that ΔH is positive. Redrawn after Miedema and de Châtel.[37]

$Q/P = 9.4$

{ Φ in volts; n_b in density units; V in cm^3; H in kJ/mol }

a) TM (NB) − TM (NB) $P = 14.1$

b) SM − SM (liquid) $P = 10.6$

c) SM − TM $P = 12.3$

The Pettifor structure map for AB compounds.

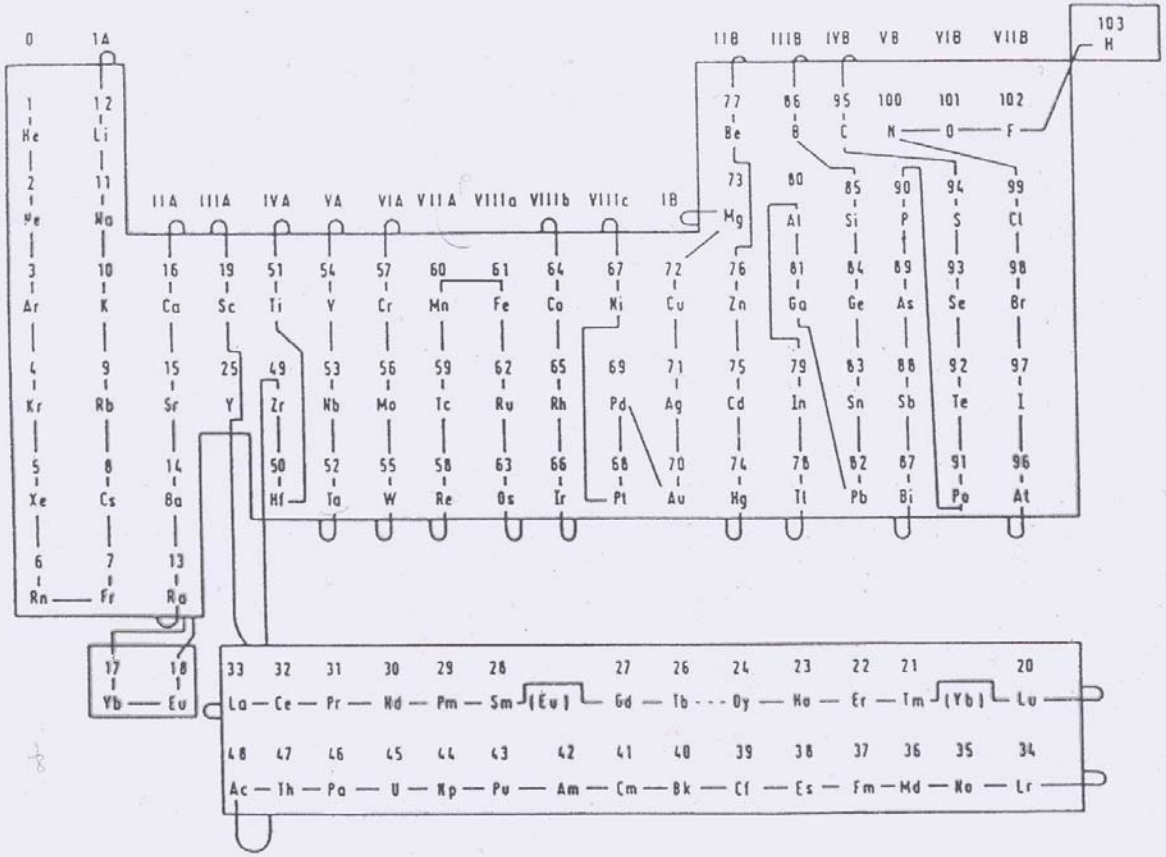

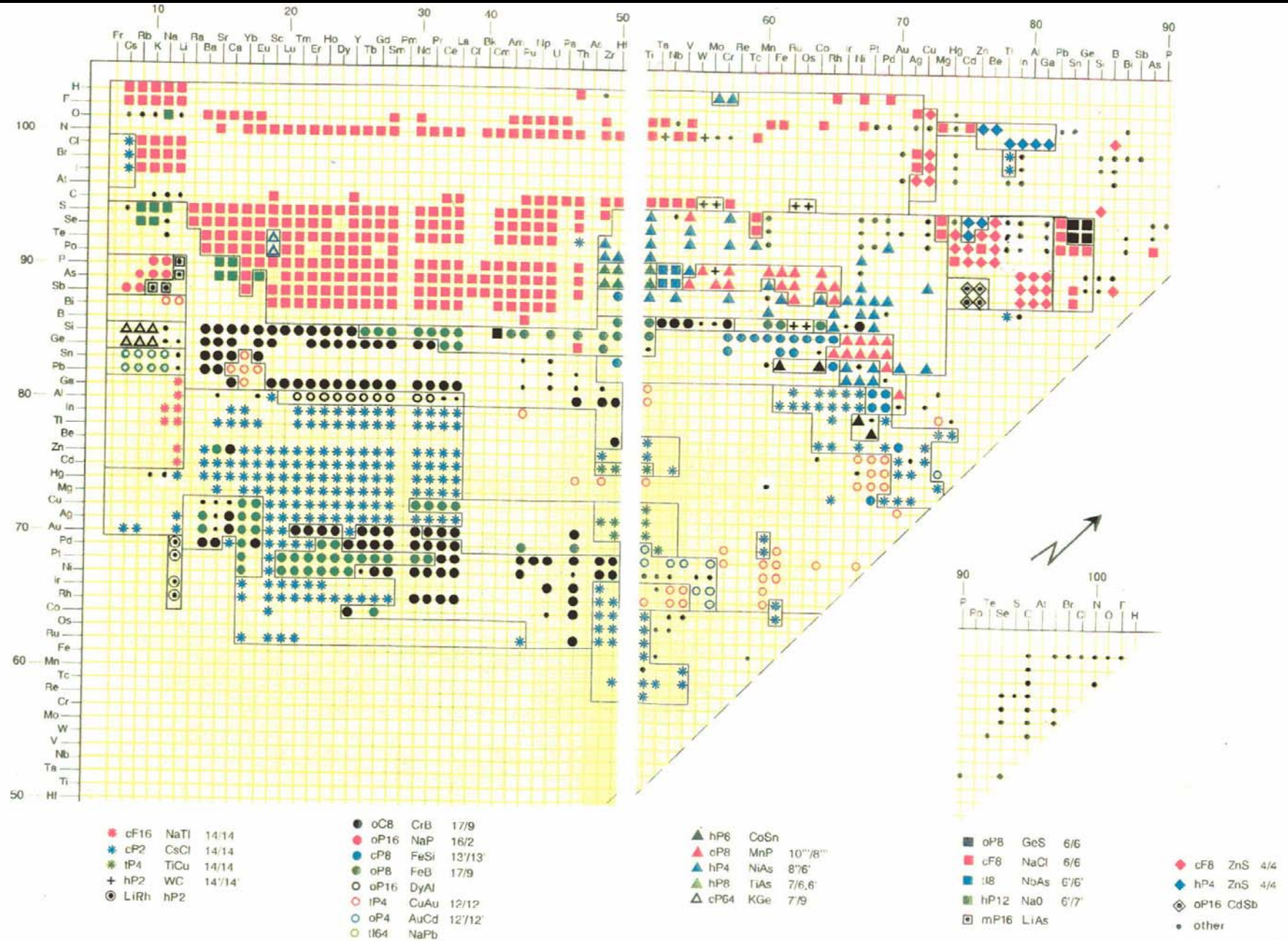
10
20
30
40
50
60
70
80
90
100
Fr Rb Na Ra Sr Yb Sc Tm Ho Y Gd Pm Pr La Ac Am Np Pa Ac Hf
Cs K Li Ba Ca Eu Lu Er Dy Tb Sm Nd Ce Cf Cm Pu U Th Zr
Ti Nb W Cr Tc Fe Os Rh Ni Pd Ag Mg Cd Be In Ga Sn Si Bi As
Ta V Mo Re Mn Ru Co Ir Pt Au Cu Hg Zn Tl Al Pb Ge B Sb P
H F O N Cl Br I At C S Se Te Po P As Sb Bi B Si Ge Sn Pb Ge Al In Tl Be Zn Cd Hg Mg Cu Ag Au Pd Pt Ni Ir Rh Co Os Ru Fe Mn Tc Re Cr Mo W V Nb Ta Ti Hf
cF16 NaTl 14/14
cP2 CsCl 14/14
tP4 TiCu 14/14
hP2 WC 14'/14'
LiRh hP2
oC8 CrB 17/9
oP16 NaP 16/2
cP8 FeSi 13'/13'
oP8 FeB 17/9
oP16 DyAl
tP4 CuAu 12/12
oP4 AuCd 12'/12'
tI64 NaPb
hP6 CoSn
cP8 MnP 10'''/8'''
hP4 NiAs 8''/6'
hP8 TiAs 7/6,6'
cP64 KGe 7'/9
oP8 GeS 6/6
cF8 NaCl 6/6
tI8 NbAs 6'/6'
hP12 Na0 6'/7'
mP16 LiAs
cF8 ZnS 4/4
hP4 ZnS 4/4
oP16 CdSb
other

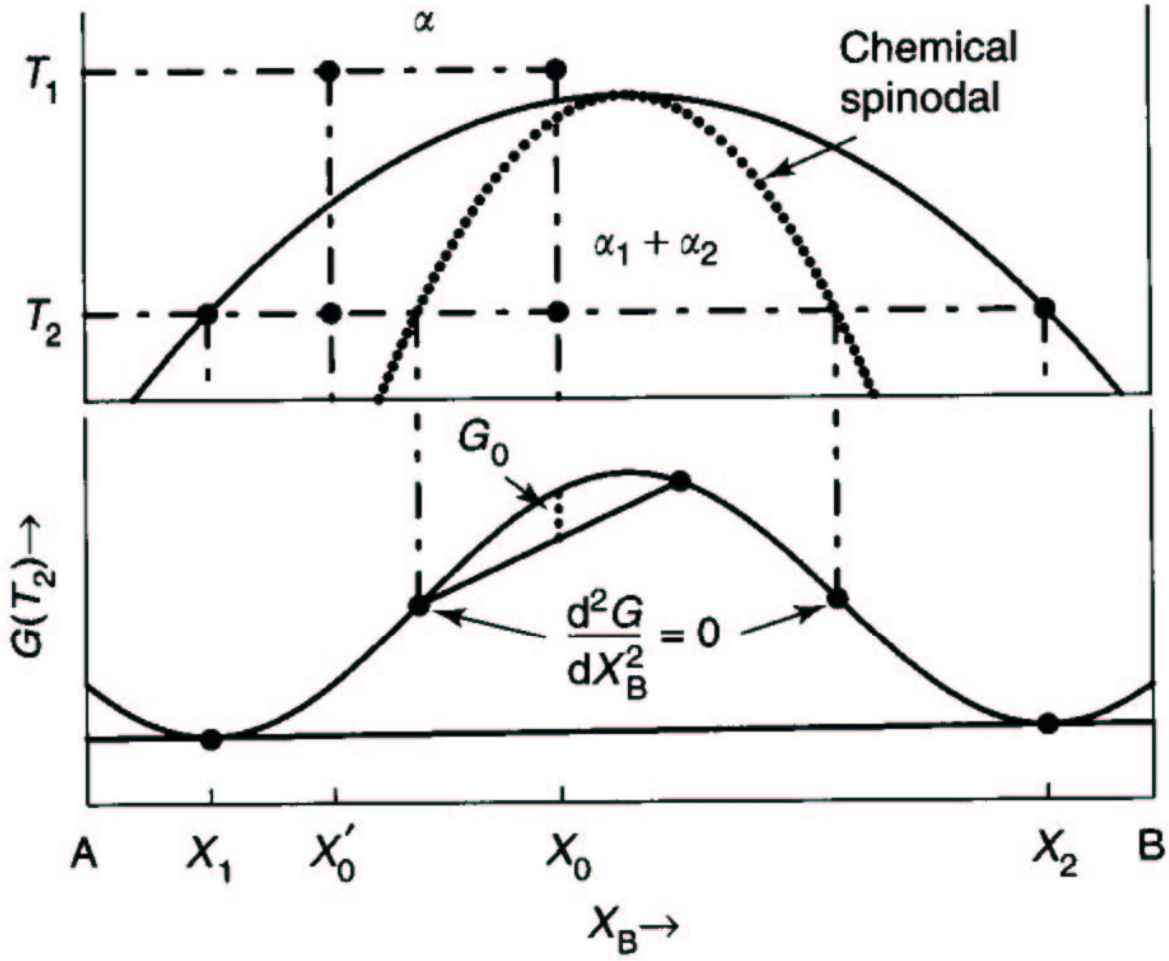

Gibbs free energy

$$G = E + PV - TS$$

Chemical potential

$$\mu_I = \left(\frac{\partial G}{\partial n_I} \right)\Bigg|_{T.P, n_{J \neq I}}$$

Gibbs-Duhem relation

$$SdT - VdP + \sum_I n_I d\mu_I = 0$$

$$F = -k_B T \ln Z \qquad Z = \sum_s \exp\left(-\frac{E_s}{kT} \right)$$

Model:

Consider a complex solution phase $(A_{x_A^{(1)}} D_{x_D^{(1)}} V_{x_V^{(1)}})(B_{x_B^{(2)}} A_{x_A^{(2)}} E_{x_E^{(2)}})(C_{x_C^{(3)}} D_{x_D^{(3)}} V_{x_V^{(3)}})$

based at a complex compound $A_k B_l C_m$

We will represent any type of species as J (J=A, B, C), their fractions at sublattice *s* as $x_J^{(s)}$ and the stoichiometric coefficients for the sublattice (or more correctly, the multiplicity of the sublattice in the $A_k B_l C_m$ phase) as $n^{(s)}$ ($n^{(s)} = k,l,m$).

Concentration, mixing entropy, and and mixing enthalpy:

$$\sum_s n^{(s)} x_J^{(s)} = c_J \sum_s n^{(s)} (1 - x_{Vac}^{(s)})$$

$$\Delta S_{mix} = -k_B \sum_s n^{(s)} \sum_J x_J^{(s)} \ln(x_J^{(s)})$$

$$\Delta H_{mix} = H_{solution} - \left[\sum_s n^{(s)} (1 - x_{Vac}^{(s)}) \right] \left[\sum_J c_J H_J \right]$$

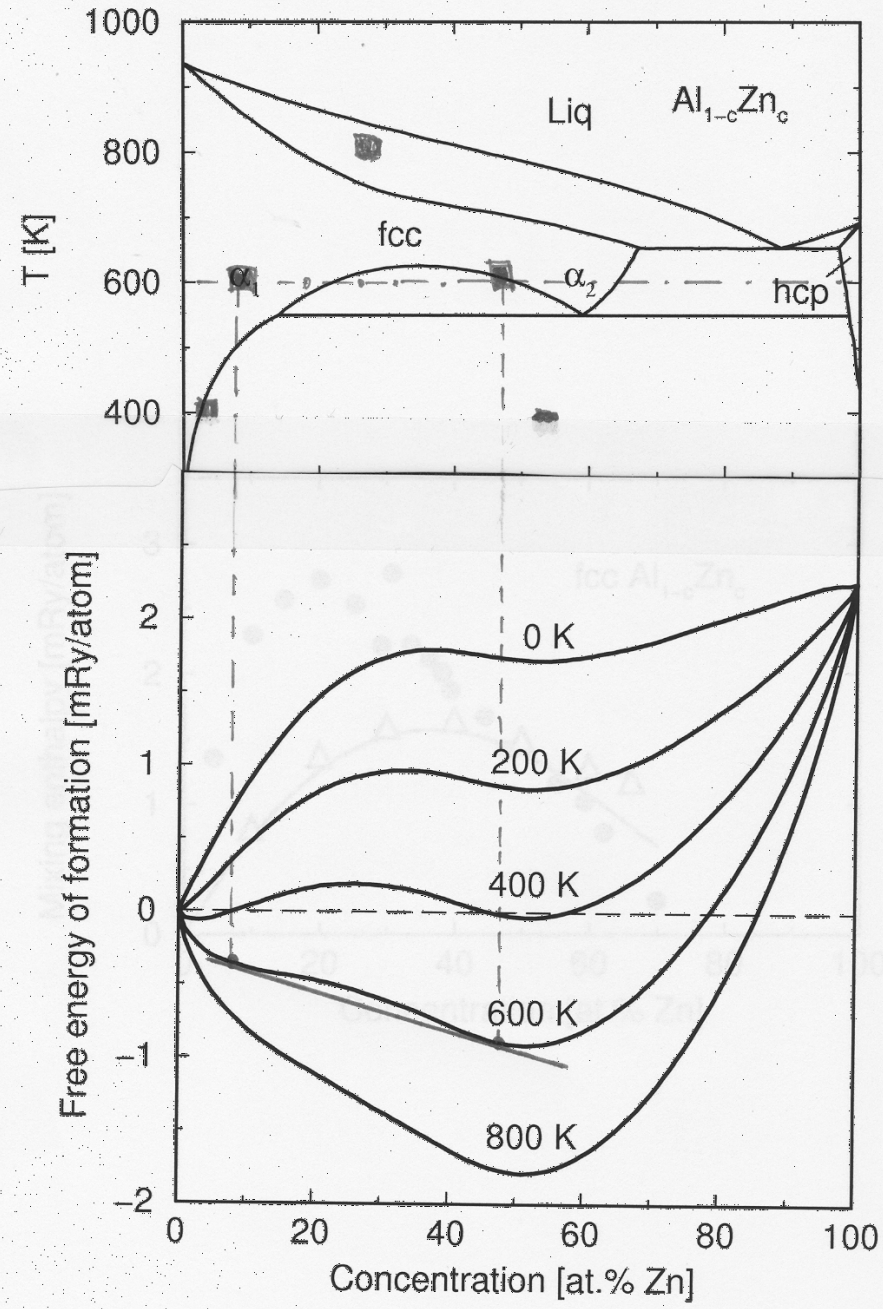
1000
800
600
400
T [K]
Liq
$Al_{1-c}Zn_c$
fcc
α_2
hcp
2
1
0
−1
−2
Free energy of formation [mRy/atom]
0 K
200 K
400 K
600 K
800 K
0
20
40
60
80
100
Concentration [at.% Zn]

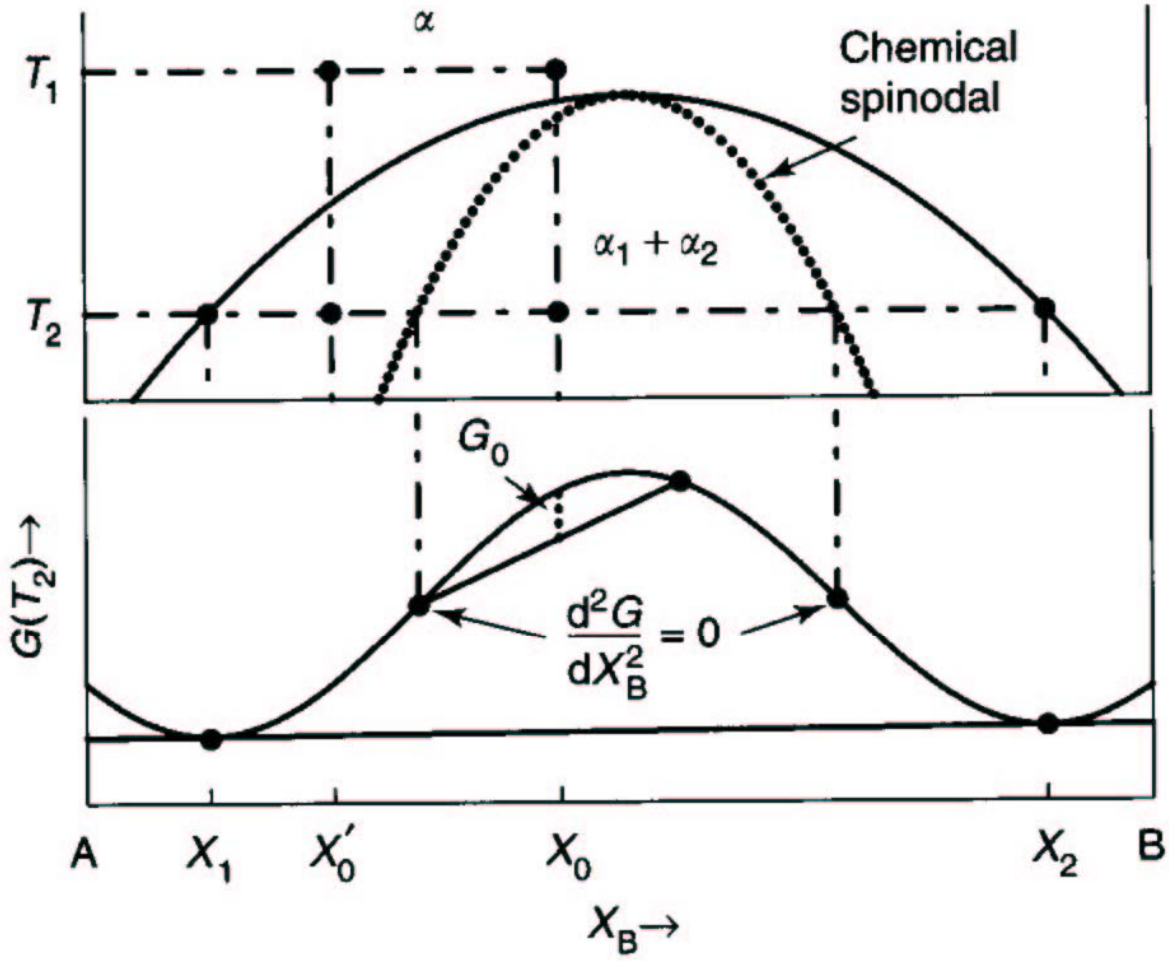

Gibbs free energy

$$G = E + PV - TS$$

Chemical potential

$$\mu_I = \left(\frac{\partial G}{\partial n_I} \right)\Bigg|_{T.P, n_{J \neq I}}$$

Gibbs-Duhem relation

$$SdT - VdP + \sum_I n_I d\mu_I = 0$$

$$F = -k_B T \ln Z \qquad Z = \sum_s \exp\left(-\frac{E_s}{kT} \right)$$

Kohn-Sham Hamiltonian

$$
\begin{cases}
H_{KS}\phi_i^{\sigma}(r,\mathrm{R}_1,\mathrm{R}_2,\ldots\mathrm{R}_{\mathrm{M}}) = \varepsilon_i^{\sigma}\phi_i^{\sigma}(r,\mathrm{R}_1,\mathrm{R}_2,\ldots\mathrm{R}_{\mathrm{M}}) \\
H_{KS} = -\frac{1}{2}\nabla^2 + V_{KS}^{\sigma}[n(r,\mathrm{R}_1,\mathrm{R}_2,\ldots\mathrm{R}_{\mathrm{M}})] \\
V_{KS}^{\sigma}[n(r,\mathrm{R}_1,\mathrm{R}_2,\ldots\mathrm{R}_{\mathrm{M}})] = V_H[n] + V_{EXT}[n] + V_{XC}^{\sigma}[n] + V_{Mad} \\
n(r,\mathrm{R}_1,\mathrm{R}_2,\ldots\mathrm{R}_{\mathrm{M}}) = \sum_{\sigma} n^{\sigma}(r,\mathrm{R}_1,\mathrm{R}_2,\ldots\mathrm{R}_{\mathrm{M}}) = \sum_{\sigma}\sum_{occ}\phi_i^{\sigma *}\phi_i^{\sigma}
\end{cases}
$$

Generalized Ising Hamiltonian

$$H_{conf} = \frac{1}{2}\sum_p V_p^{(2)}\sum_{i,j\in p}\sigma_i\sigma_j + \frac{1}{3}\sum_t V_t^{(3)}\sum_{i,j,k\in t}\sigma_i\sigma_j\sigma_k + \ldots$$

$$\Phi_f^{(n)}(\sigma) = \prod_{i\in f}\sigma_i$$

$$V_f^{(n)} = \left\langle E_{tot}(\sigma)\Phi_f^{(n)}(\sigma)\right\rangle$$

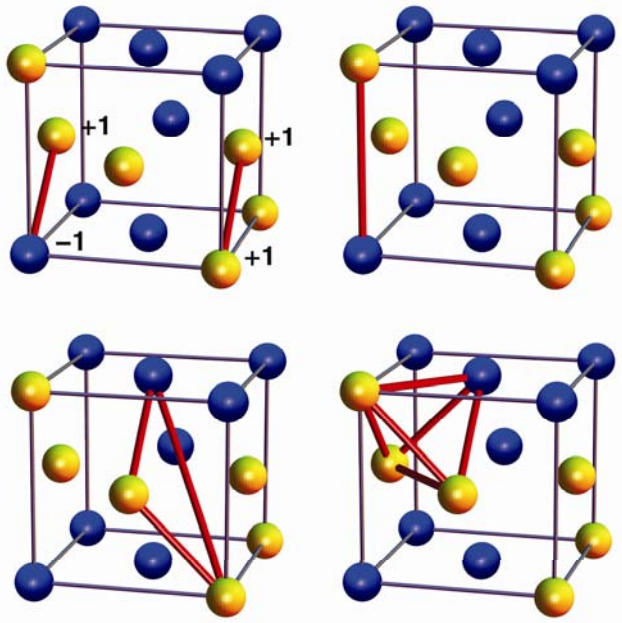

$$\mathrm{E}[n] = \mathrm{T} + \int d^3\vec{\mathrm{r}}\,V_{EXT}(\vec{\mathrm{r}})n(\vec{\mathrm{r}}) + \int d^3\vec{\mathrm{r}}\,n(\vec{\mathrm{r}})\left[\frac{1}{2}\int d^3\vec{\mathrm{r}}'\frac{n(\vec{\mathrm{r}}')}{|\vec{\mathrm{r}}-\vec{\mathrm{r}}'|}\right] + \mathrm{E}_{\mathrm{II}} + \mathrm{E}_{\mathrm{XC}}[n^{\uparrow},n^{\downarrow}] = \sum_f V_f^{(n)}\Phi_f^{(n)}(\sigma) = E(\sigma)$$

A. V. Ruban and I. A. Abrikosov, Rep. Prog. Phys. 71, 046501 (2008).

For a fixed alloy concentration, i.e. in the canonical ensemble, the configurational Hamiltonian is frequently written in terms of *fluctuations* of either spin- or concentration variables, $\delta c_i = c_i - c$:

$$H_{conf} = \frac{1}{2}\sum_p \tilde{V}_p^{(2)} \sum_{i,j\in p} \delta c_i \delta c_j + \frac{1}{3}\sum_t \tilde{V}_t^{(3)} \sum_{i,j,k\in t} \delta c_i \delta c_j \delta c_k + \ldots . \tag{59}$$

Here $\tilde{V}_f^{(n)}$ $(f = p, t, ...)$ are the interactions in the concentration-variable basis, which are connected to the interactions in the spin-variable basis as $\tilde{V}_f^{(n)} = 2^n V_f^{(n)}$. If the pair interactions $\tilde{V}_p^{(2)}$ are dominating in the system it is very convenient to use a reciprocal-space representation of the ordering energy for a general analysis of the ordering [103, 3, 8]

$$H_{conf} = \frac{1}{2}\sum_{\mathbf{k}} \tilde{V}(\mathbf{k}) \mid c_{\mathbf{k}} \mid^2 . \tag{60}$$

Here $\tilde{V}(\mathbf{k})$ and $c_{\mathbf{k}}$ are the Fourier transforms of $\tilde{V}_p^{(2)}$ and δc_i, respectively:

$$\tilde{V}(\mathbf{k}) = \sum_p \tilde{V}_p^{(2)} \sum_{\mathbf{R}\in p} e^{-i\mathbf{k}\mathbf{R}}, \tag{61}$$

$$c_{\mathbf{k}} = \frac{1}{N}\sum_i \delta c_i e^{-i\mathbf{k}\mathbf{R}_i}. \tag{62}$$

In the case of a binary A_cB_{1-c} alloy

$$|c_{\mathbf{k}}|^2 = c(1-c)\alpha_{\mathbf{k}}.$$

well-known Krivoglaz-Clapp-Moss formula

$$\alpha(\mathbf{k}) = \left[1 + c(1-c)\beta V(\mathbf{k})\right]^{-1},$$

Extrapolation vs interpolation

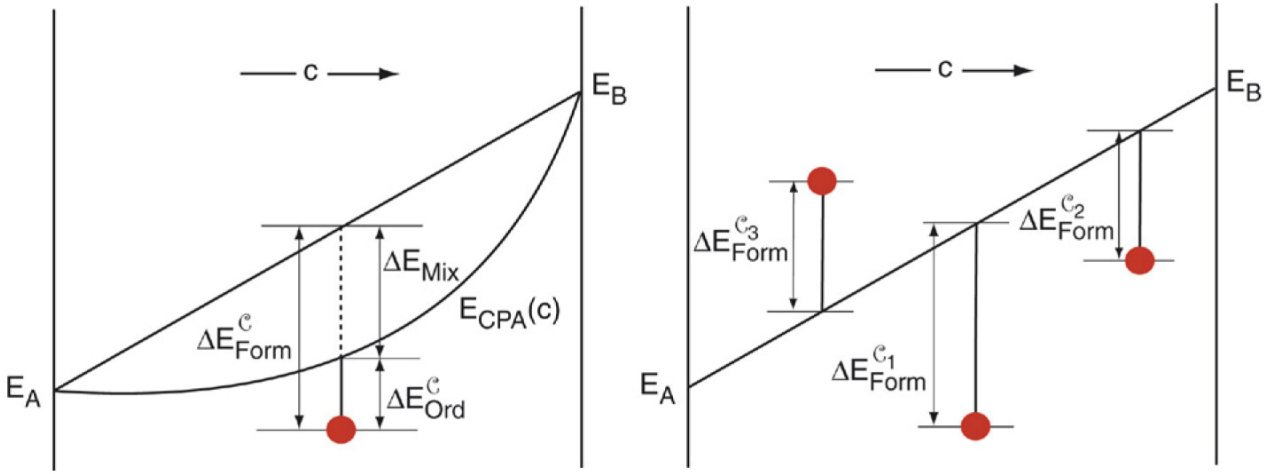

Fig. 5. (Color online) Schematic representations of the two categories of methods that are used to describe chemical order in alloys (see text for details). In the right panel, the "C_i" refer to particular chemical configurations of the alloy.

Calculations of effective interatomic potentials

The Connolly-Williams method

1. Select structures

fcc **$L1_2$** **$L1_0$** **DO22**

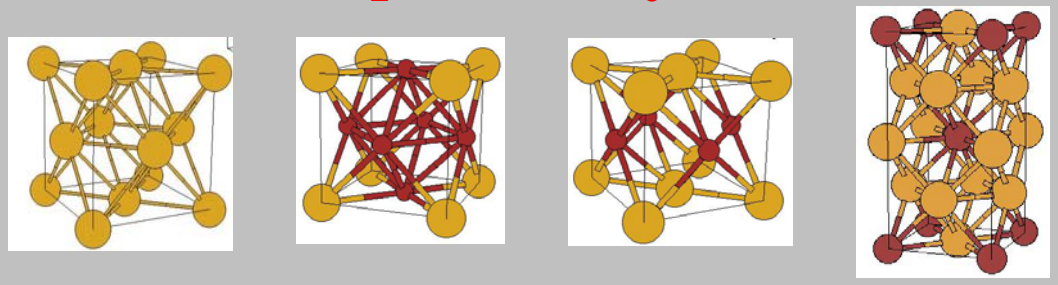

with predefined correlation functions

$$\left[\left\langle \sigma_i\sigma_j \right\rangle^{(2,1)}, \left\langle \sigma_i\sigma_j \right\rangle^{(2,2)}, \left\langle \sigma_i\sigma_j\sigma_k \right\rangle^{(3,1)}, \ldots\right]$$

2. Calculate E_{tot}: **E(fcc)** **E($L1_2$)** **E($L1_0$)** **E(DO22)**

$$E_{tot} = V^{(0)} + V^{(1)}\left\langle \sigma \right\rangle + \sum_s V^{(2,s)}\left\langle \sigma_i\sigma_j \right\rangle \ldots$$

If $N_{pot} \le N_{str}$ then $\{V\}$ are found by L.S.M : $\sum_m \left[E_m - \sum_f \left\langle \ldots \right\rangle^f V_f \right]^2 = \min$

Direct cluster averaging method

A closer inspection of definition (45) for the ECI reveals that they can be rewritten in a more transparent form, as suggested by Berera *et al.* [186, 187] in the so-called direct cluster averaging (DCA) method. For instance, the ECI in the case of a binary A_cB_{1-c} alloy is [186, 187]: $V_s^{(n)} = \left\langle E_{tot}(\sigma)\Phi_s^{(n)}(\sigma)\right\rangle$

$$V_s^{(n)} = \frac{1}{2^n} \sum_{\sigma_1,\sigma_2\ldots\sigma_n=1,-1} v_s^{(n)}(\{\sigma_1,\sigma_2,\ldots\sigma_n\}) \prod_{\sigma_{i=1,n}} \sigma_i, \tag{68}$$

where $v_s^{(n)}(\{\sigma_1,\sigma_2,\ldots\sigma_n\})$ are the n-body potentials of cluster s composed of A and B atoms in the configuration $\{\sigma_1,\sigma_2,\ldots\sigma_n\}$, and the summation is over all possible occupations of this cluster. It is determined as the total energy of the system averaged over all the remaining configurations under given external and internal conditions:

$$v_s^{(n)}(\{\sigma_1,\sigma_2,\ldots\sigma_n\}) = \frac{1}{z}\sum_{\sigma} E(\{\sigma_1,\sigma_2,\ldots\sigma_n\}_s;\sigma). \tag{69}$$

Here $E(\{\sigma_1,\sigma_2,\ldots\sigma_n\}_s;\sigma)$ is the energy of a system having configuration $\{\sigma_1,\sigma_2,\ldots\sigma_n\}_s$ in the cluster s and σ in the rest of the system; z is the total number of configurations, which in the case of concentration-independent ECI determined on the N-site system is 2^{N-n}. A similar expressions can be written for multicomponent systems [188]. However, it is clear, that it is practically impossible to use Eq. (69) in first-principles calculations without either sever restrictions on the size of the system or indroducing additional approximations. Berera *et al.* [186, 187], for instance, used a real-space tight-binding formalism in order to calculate the ECI by the DCA.

Generalized Perturbation Method (GPM)

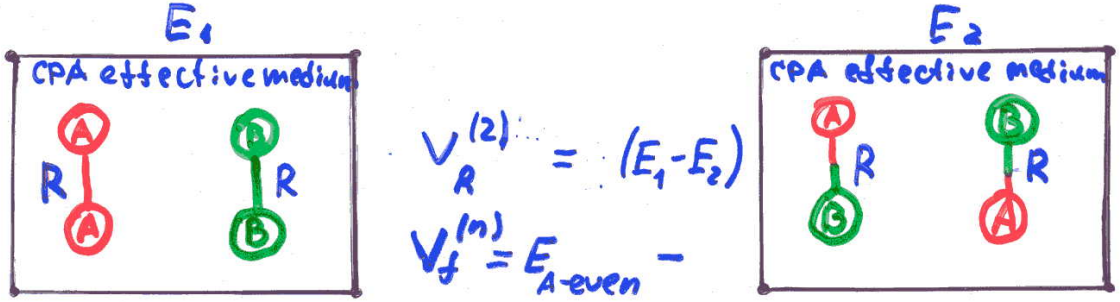

$$V_R^{(2)} = (E_1 - E_2)$$

$$V_f^{(n)} = E_{A\text{-even}} - E_{A\text{-odd}}$$

Andersen force theorem: The change in energy between two systems is given to the first approximmation by the change in one-electron energy and the change in the electrostatic interaction due to the perturbation

KKR-ASA:

$$V_{one\text{-}el}^{(2,R)} = -\frac{1}{\pi} Im \int^{E_F} Tr\,[\Delta t_0\, \tilde{g}_{0R}\, \Delta t_R\, \tilde{g}_{R0}]\, dE$$

where $\tilde{g}$ is the effective medium Green's function (e.g. CPA), $\Delta t_i = t_i^A - t_i^B$, and t is the scattering matrix for a single site in the system: $t_i = [1 + (\tilde{m} - m_i)\tilde{g}_{00}]^{-1}(\tilde{m} - m_i)$

$$V_{electrostatic}^{(2,R)} = \frac{e^2}{2}(q_A - q_B)^2 \frac{\alpha_{scr}(R)}{R_{ws}}, \text{ where}$$

$q_{A(B)}$ is the net charge for A(B) alloy component, $\alpha_{scr}(R)$ is the intersite screening constant.

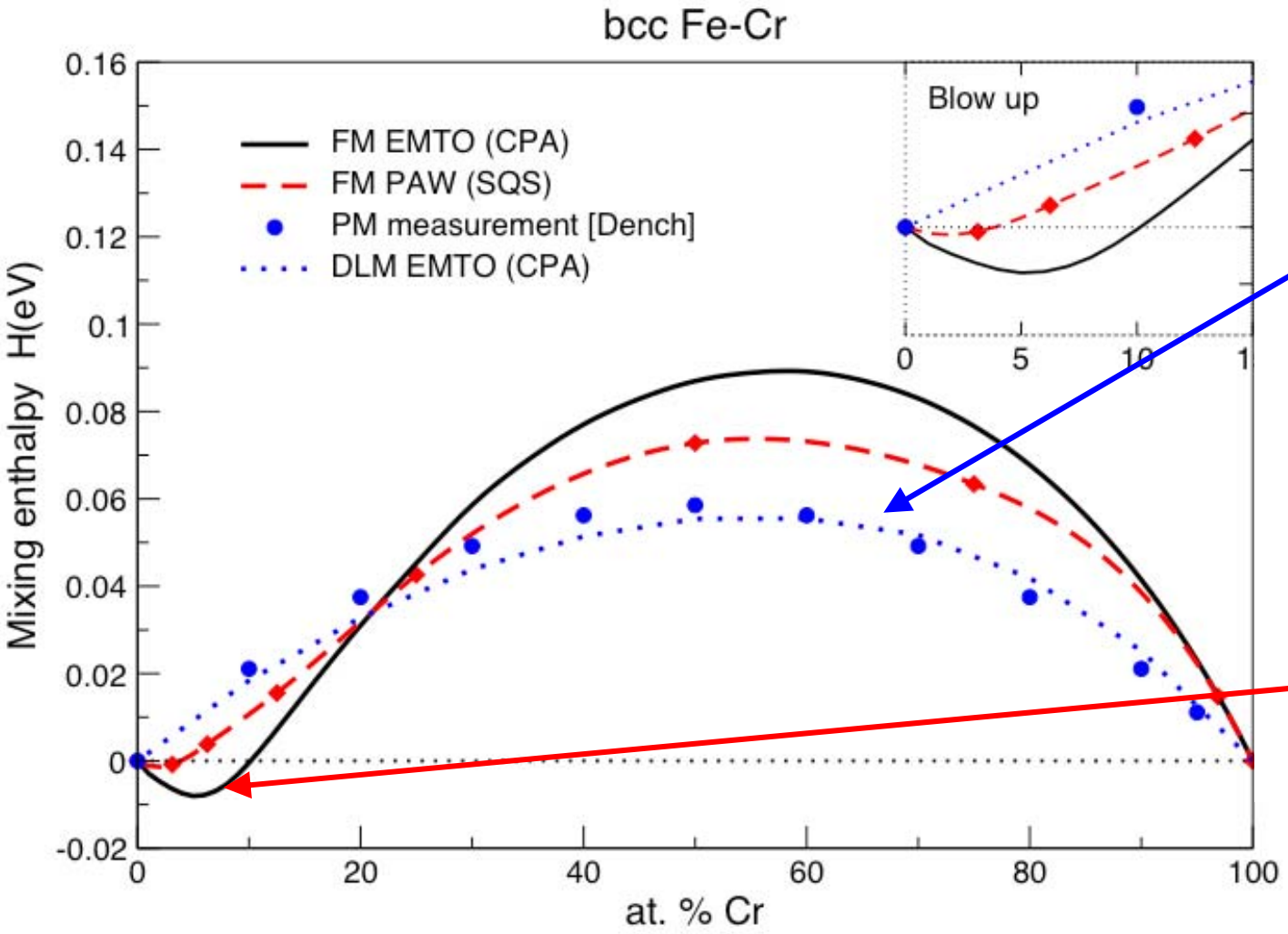

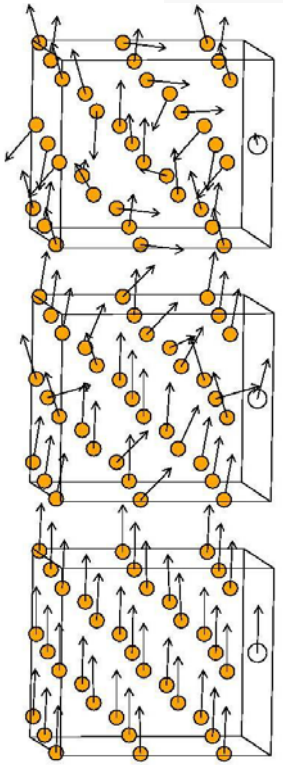

P. Olsson, I. A. Abrikosov, L. Vitos, and J. Wallenius, J. Nucl. Mater. 321, 84 (2003)

P. Olsson, I. A. Abrikosov, and J. Wallenius, Phys. Rev. B 73, 104416 (2006)

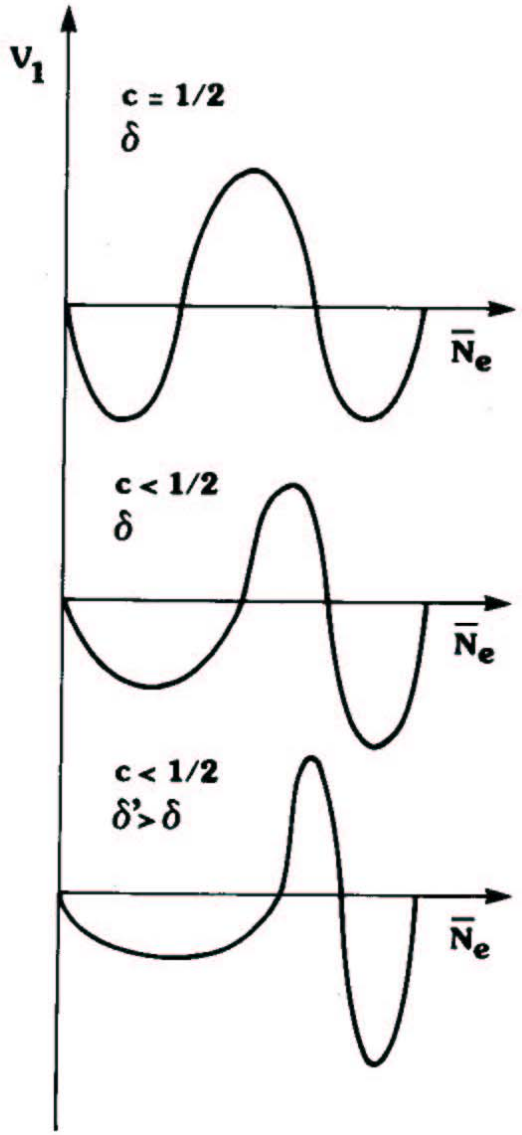

Fig. 7.5. Typical variations of $V_1(\bar{N}_e)$ for different values of c and of δ.

F. Ducastelle, Order and Phase Stability in Alloys

J. Phys. F: Met. Phys. 13 (1983) 2351–2358. Printed in Great Britain

Ab initio, this work.

Chemical SRO effects in ferromagnetic Fe alloys in relation to electronic band structure

M Hennion

Laboratoire Léon Brillouin, CEN Saclay, 91191 Gif-sur Yvette Cédex, France

Received 3 May 1983

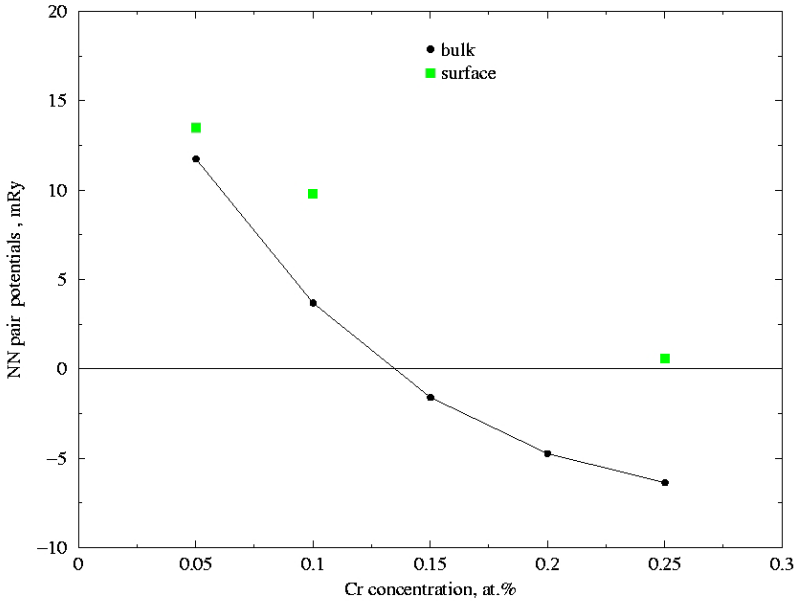

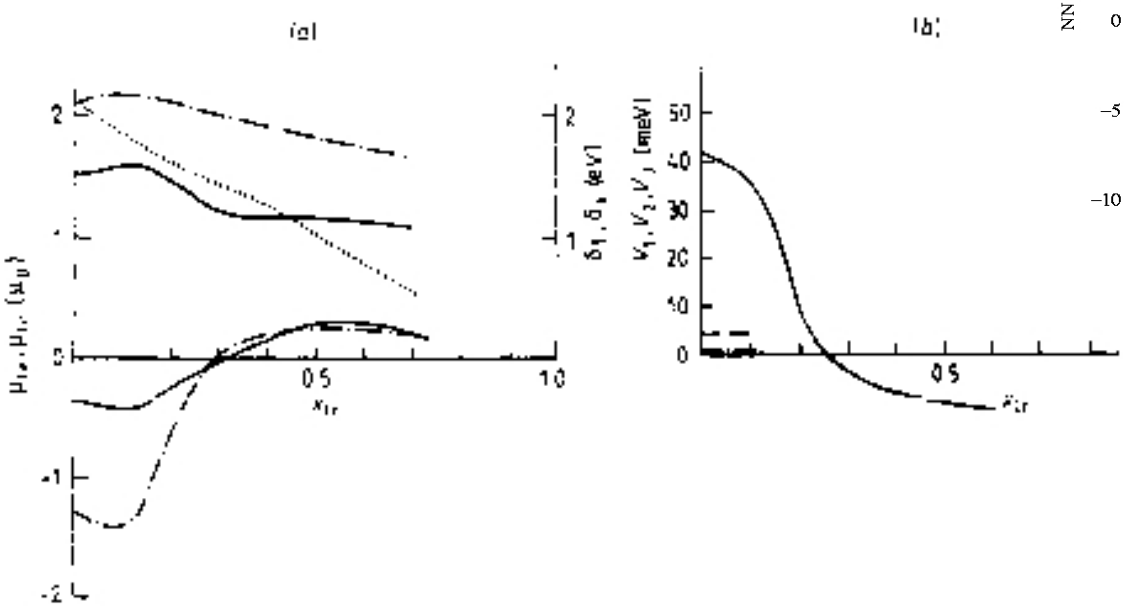

Figure 2. FeCr alloys. (*a*) Calculated curves of the partial $\mu_{Fe}(c)$ and $\mu_{Cr}(c)$ (· — · —) and total (. . .) magnetisations, and calculated curves of the energy disorder parameters δ_σ ($\sigma = \uparrow, \downarrow$) with chromium concentration (——). (*b*) Calculated variations of the pair potentials with Cr concentration: V_1(——), V_2( ) and V_3(· — · —).

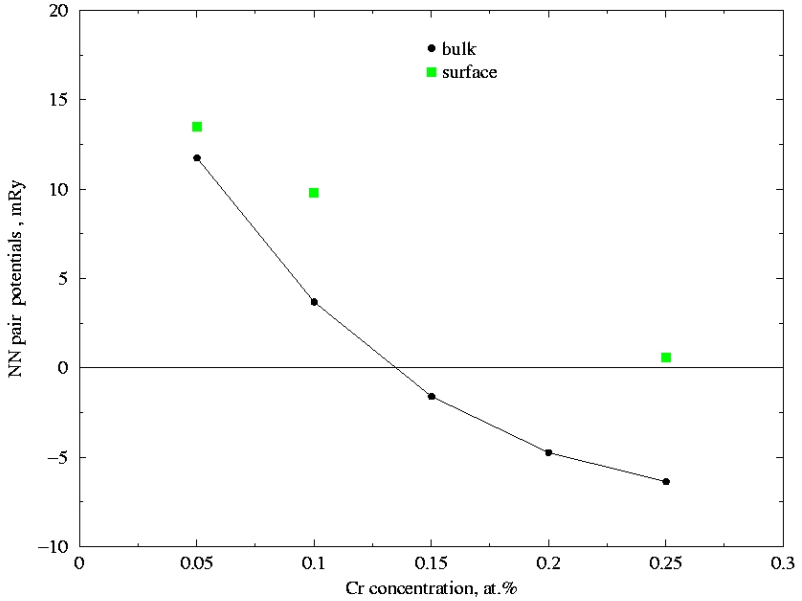
bulk
surface
NN pair potentials , mRy
Cr concentration, at.%

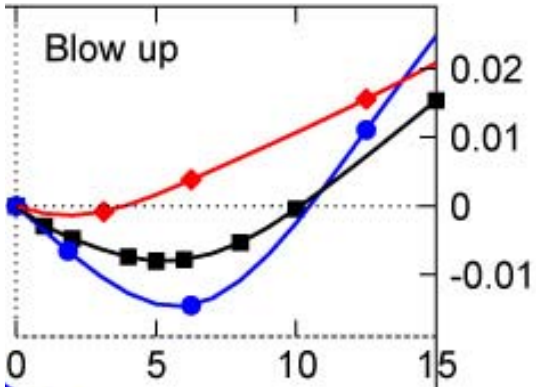
Blow up

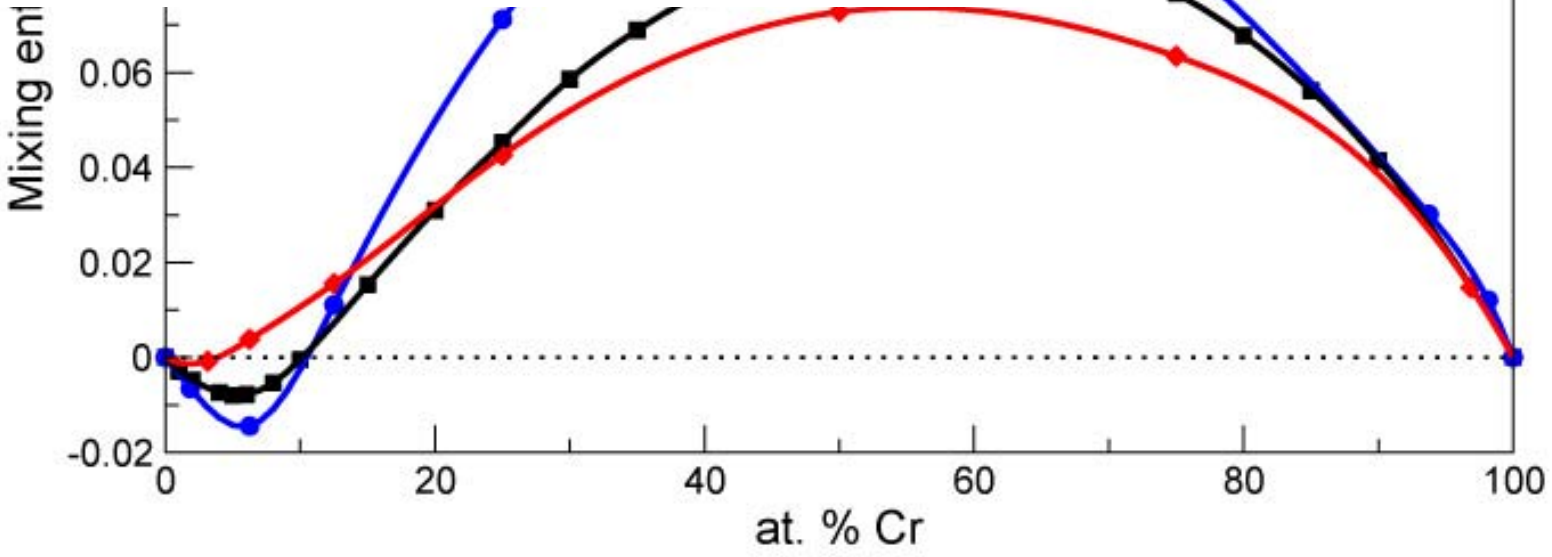
Mixing en
at. % Cr

The Monte Carlo method

Calculations of averages at temperature *T*:

$$\langle A \rangle = \frac{\sum_s A_s \exp\left(-\frac{E_s}{k_B T}\right)}{Z}$$

Create the Marcov chain of configurations:

$$P_s = \frac{1}{Z}\exp\left(-\frac{E_s}{k_B T}\right)$$

Balance at the equilibrium state:

$$W(s \to s')\exp\left(-\frac{E_s}{k_B T}\right) = W(s' \to s)\exp\left(-\frac{E_{s'}}{k_B T}\right)$$

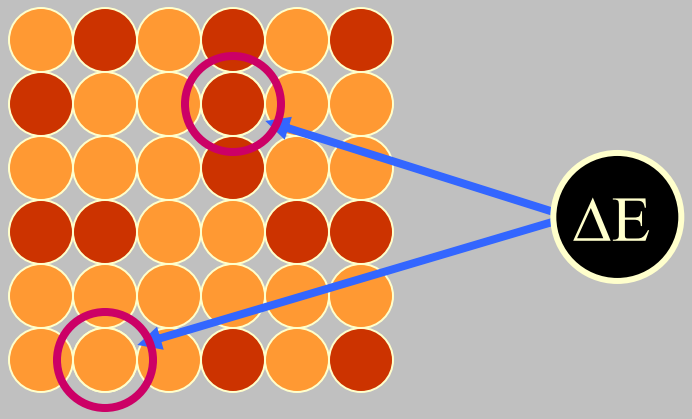

$$\begin{cases} \Delta E \le 0 \\ \Delta E > 0 \quad \exp\left[-\frac{\Delta E}{k_B T}\right] > r \quad (0 \le r \le 1) \end{cases}$$

Atoms exchanged

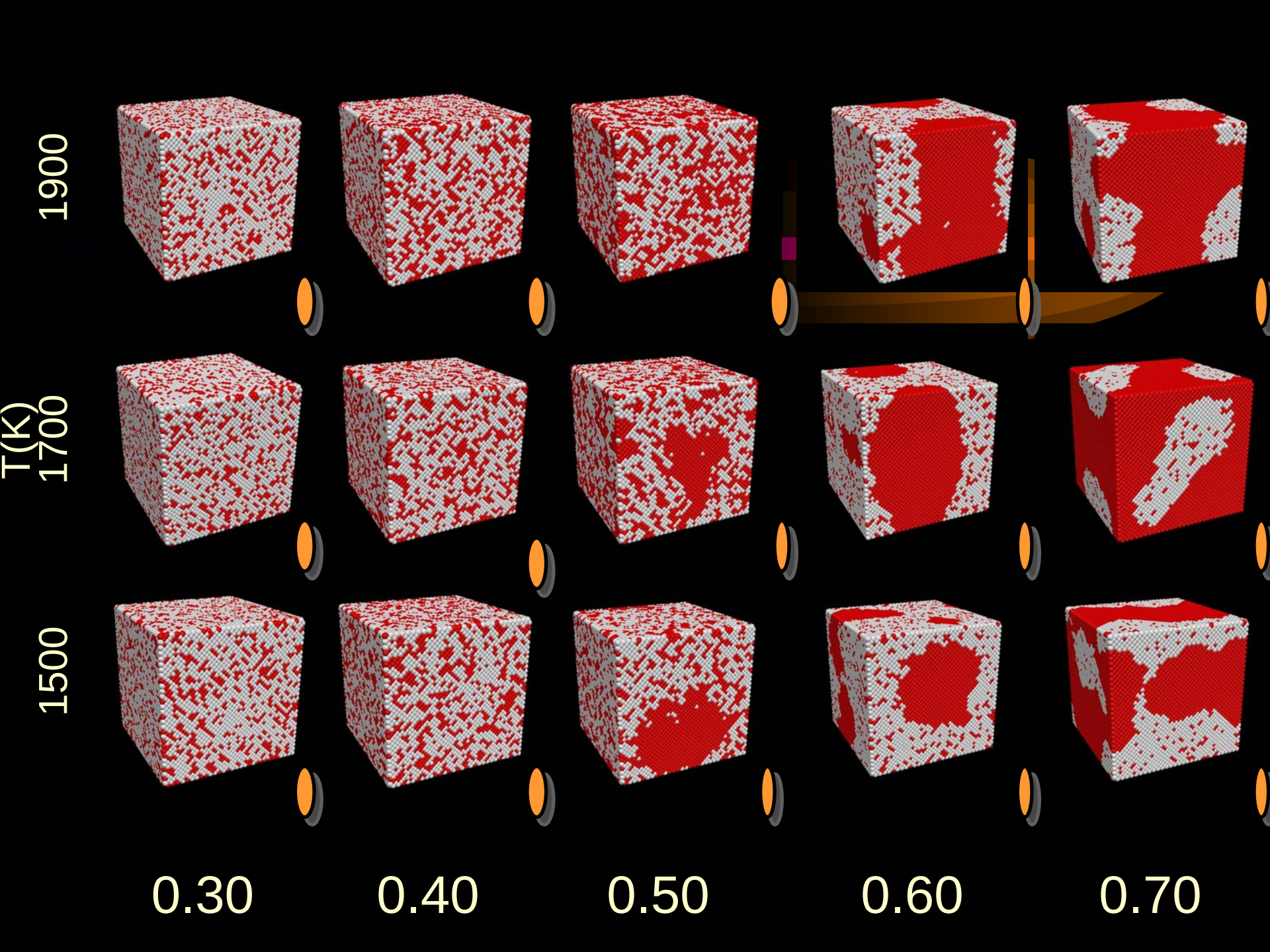
1900
T(K)
1700
1500
0.30
0.40
0.50
0.60
0.70

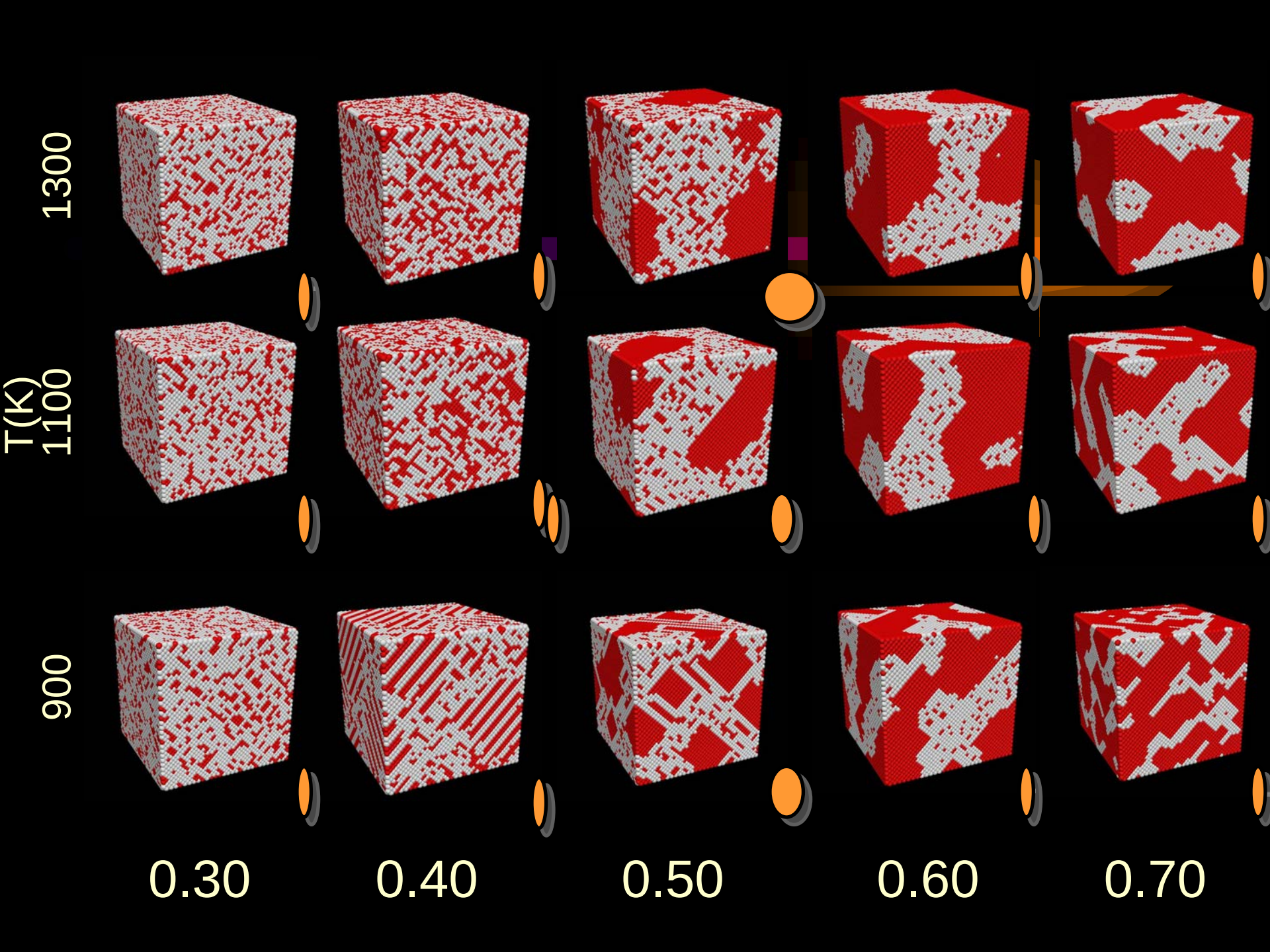
T(K)
1300
1100
900
0.30
0.40
0.50
0.60
0.70

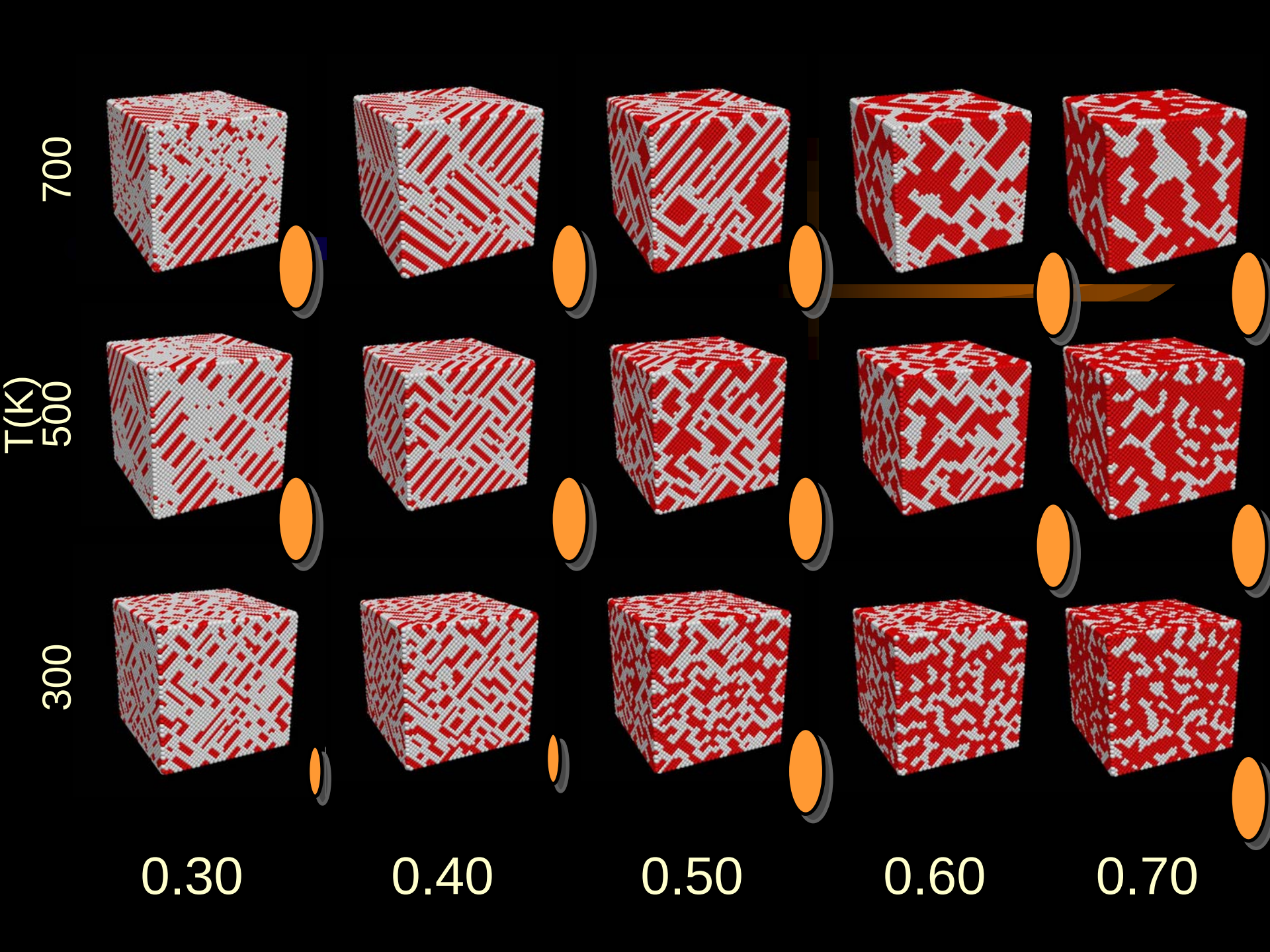
700
T(K)
500
300
0.30
0.40
0.50
0.60
0.70

Monte-Carlo method: problems

- Finite size of the samples (in general, phase transition can only be defined in the limit $N \rightarrow \infty$)
- "Kinetics" of the MC simulations: very large number of spin flips may be necessary to reach equilibrium state
- Close to a second-order phase transition the time necessary to reach equilibrium is expected to tend to infinity
- There is a possibility that the system evolves towards metastable states. It is difficult to escape from the metastable states, especially at low T.
- Hysteresis effects in the case of first-order transitions
- MC simulations are difficult in cases of frustrated systems

Example: ordered phases in Cu_2NiZn

- 21 concentration and volume dependent effective cluster interactions
- Electronic structure calculations using O(N) LSGF method
- 32 different atomic distributions at fixed concentration (144 atom supercell)
- Cluster expansion represents total energy calculations with average accuracy better than 0.015 mRy, and with the maximal error 0.2 mRy (or 4% of the ordering energy)

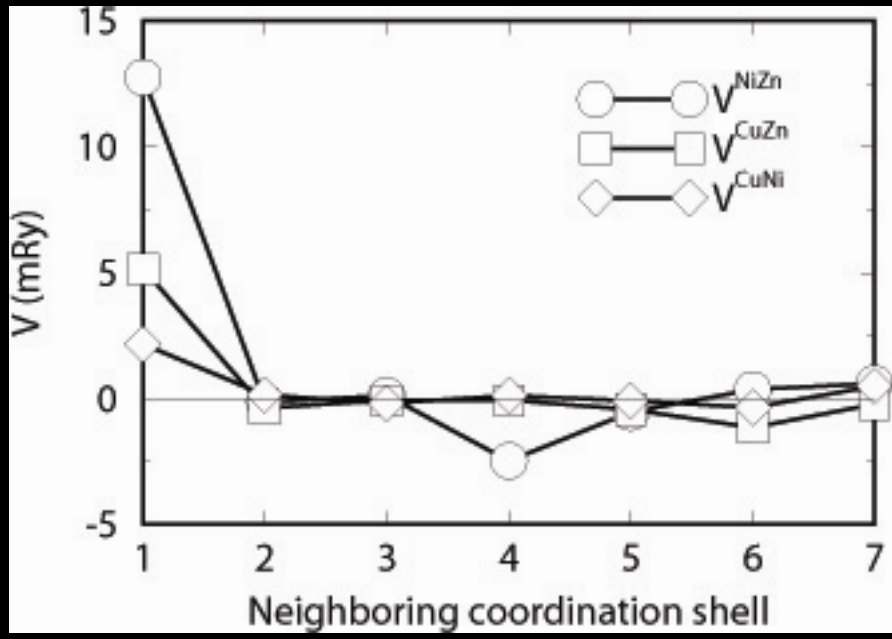

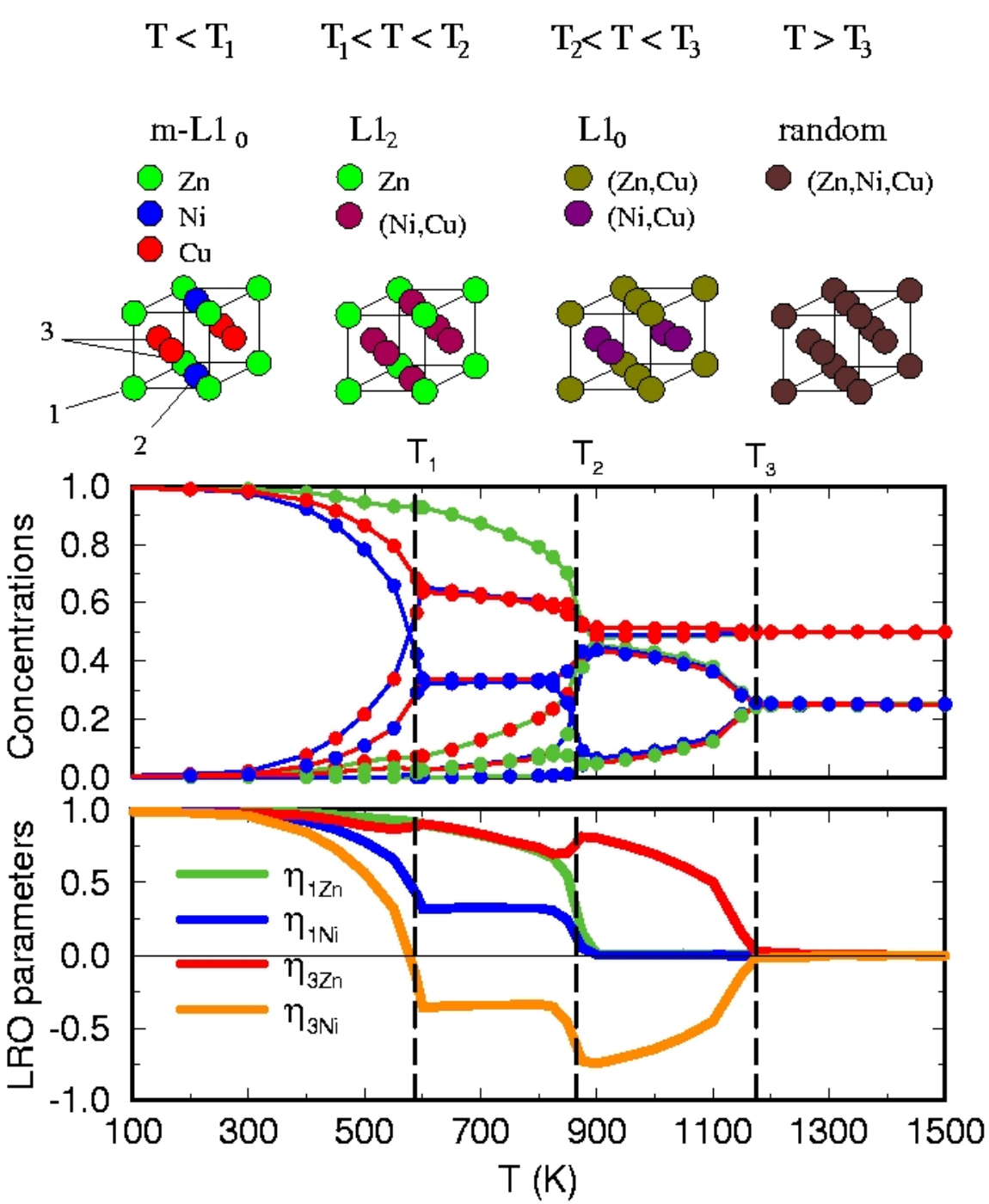

(S. I. Simak *et al.*, Phys. Rev. Lett. **81**, 188 (1998))

Magnetism and chemical interctions

Let us start from short times $\sim 10^{-13}$ sec (but long enough for d-electron-hoping ($\sim 10^{-15}$ sec)). The effective pair interactions at such time scale can be defined as the energy of the exchange of atom A in one magnetic state, say A^u with an atom B in the presence of another atom A, say A^d at some specific lattice vector $\mathbf{R}$:

$$V^{A^u A^d - B}(\mathbf{R}) = v_{A^u A^d}(\mathbf{R}) + v_{BB}(\mathbf{R}) - v_{A^u B}(\mathbf{R}) - v_{B A^d}(\mathbf{R}), \tag{78}$$

where $v_{AB}(\mathbf{R})$ is the interatomic potential between A and B atoms. There are in general three different effective interactions of such type in this case: $V^{A^u A^d - B}$ (or equivalently $V^{A^d A^u - B}$), $V^{A^u A^u - B}$, and $V^{A^d A^d - B}$. On a longer time scale they will be averaged out, one therefore gets only one effective pair interaction of an effective binary alloy $<\mathrm{A}>_c \mathrm{B}_{1-c}$:

$$V^{DLM}(\mathbf{R}) \equiv V^{<A>B}(\mathbf{R}) = \frac{1}{2}\left[V^{A^u A^d - B}(\mathbf{R}) + V^{A^u A^u - B}(\mathbf{R})\right], \tag{79}$$

where we have used the fact that $V^{A^u A^u - B} = V^{A^d A^d - B}$ in the DLM state.

$$H = -\sum_{i,j\neq i} J_{ij} s_i s_j \qquad V^{DLM}(\vec{R}) = V^{FM}(\vec{R}) + 2J^{AA}(\vec{R})$$

Exchange parameters

Pair exchange parameter

$\frac{\Theta}{2}$

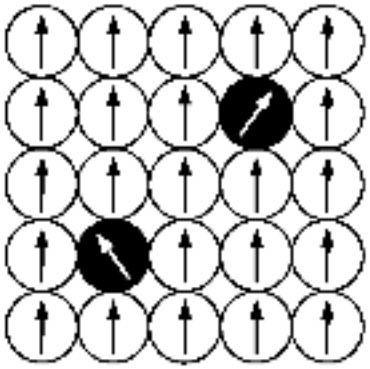

i

j

$J_{ij} > 0$ ↑↑

< 0 ↑↓

Effective exchange parameter

Θ

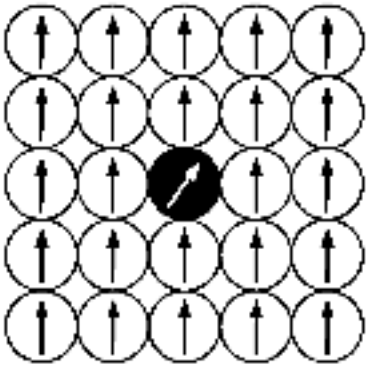

i = 0

$$J_0 = \sum_{j\neq 0} J_{0j}$$

Fe-Si system:

- At ambient pressure the phase diagram of Fe-Si system is complicated with different intermediate phases present.
- Moroni *et al. (*Phys. Rev. B **59,** 12860–12871, 1999) predicted the *B20* to *B2* structural transformation in FeSi at relatively low pressure.
- Fe_3Si phase in the DO3 structure is stabilized by the ferromagnetic order.
- J.-F. Lin *et al.,* Iron-silicon alloy in Earth's core? *Science* **295**, 313-315 (2002).
- L. Dubrovinsky *et al.*, "Iron-silica interaction at extreme conditions and the electrically conducting layer at the base of Earth's mantle", Nature **422**, 58 (2003)

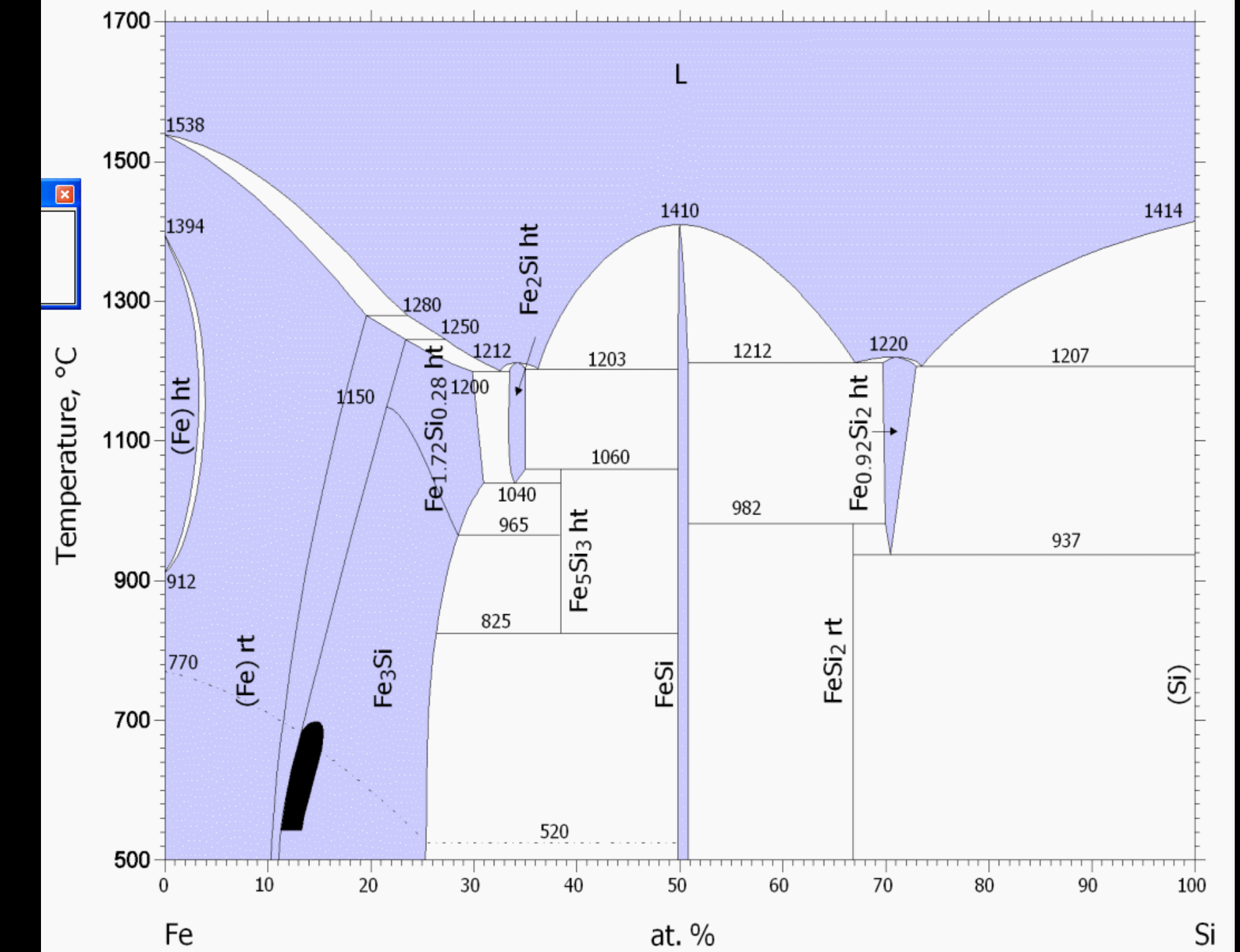
L
1538
1394
1280
1250
1212
1200
1150
1410
1414
1203
1212
1220
1207
1060
1040
965
982
937
912
825
770
520
(Fe) ht
(Fe) rt
Fe3Si
Fe1.72Si0.28 ht
Fe2Si ht
Fe5Si3 ht
FeSi
Fe0.92Si2 ht
FeSi2 rt
(Si)
Temperature, °C
1700
1500
1300
1100
900
700
500
0
10
20
30
40
50
60
70
80
90
100
Fe
at. %
Si

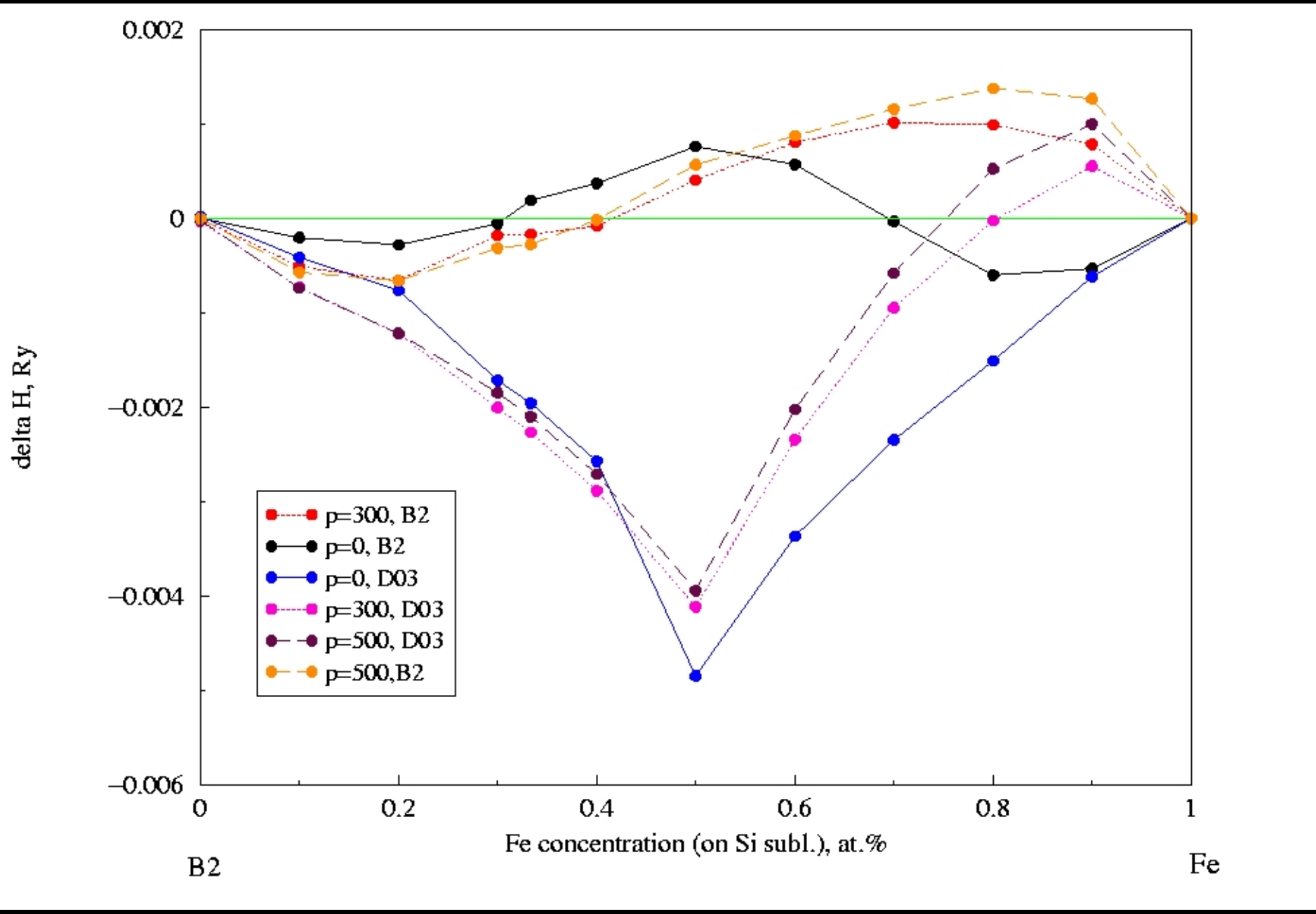
0.002
0
−0.002
−0.004
−0.006
delta H, Ry
p=300, B2
p=0, B2
p=0, D03
p=300, D03
p=500, D03
p=500,B2
0
0.2
0.4
0.6
0.8
1
Fe concentration (on Si subl.), at.%
B2
Fe

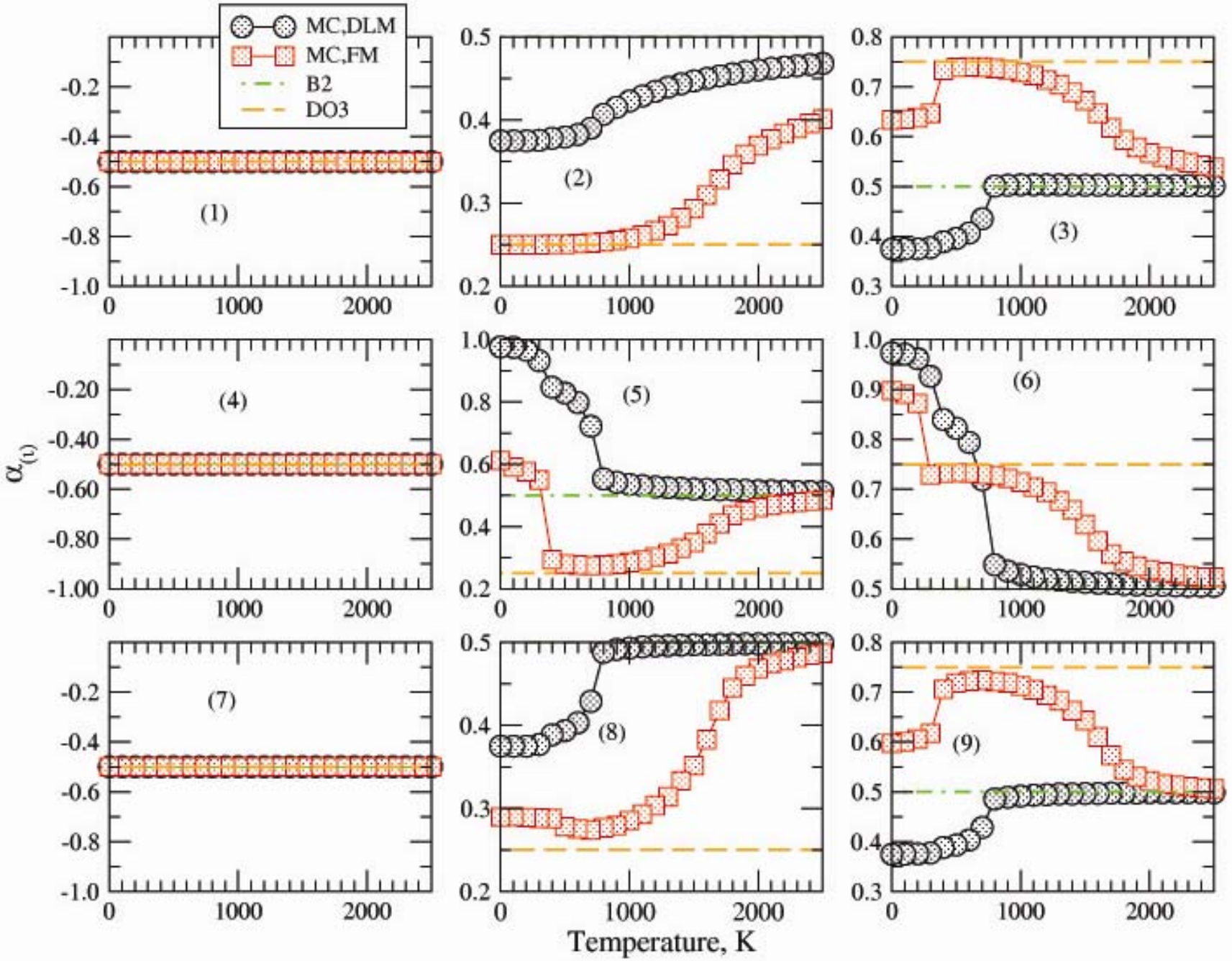
MC,DLM
MC,FM
B2
DO3
(1)
(2)
(3)
(4)
(5)
(6)
(7)
(8)
(9)
$\alpha_{(i)}$
Temperature, K

Monte-Carlo simulations: results

T=0K

T=2500 K

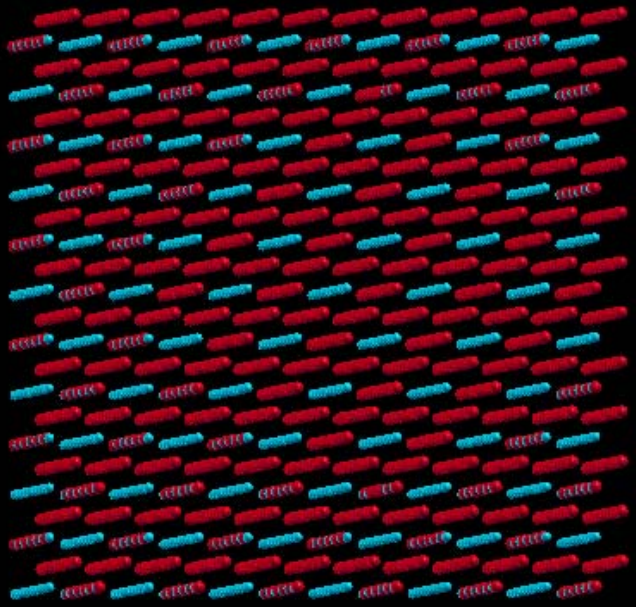

FM

DLM

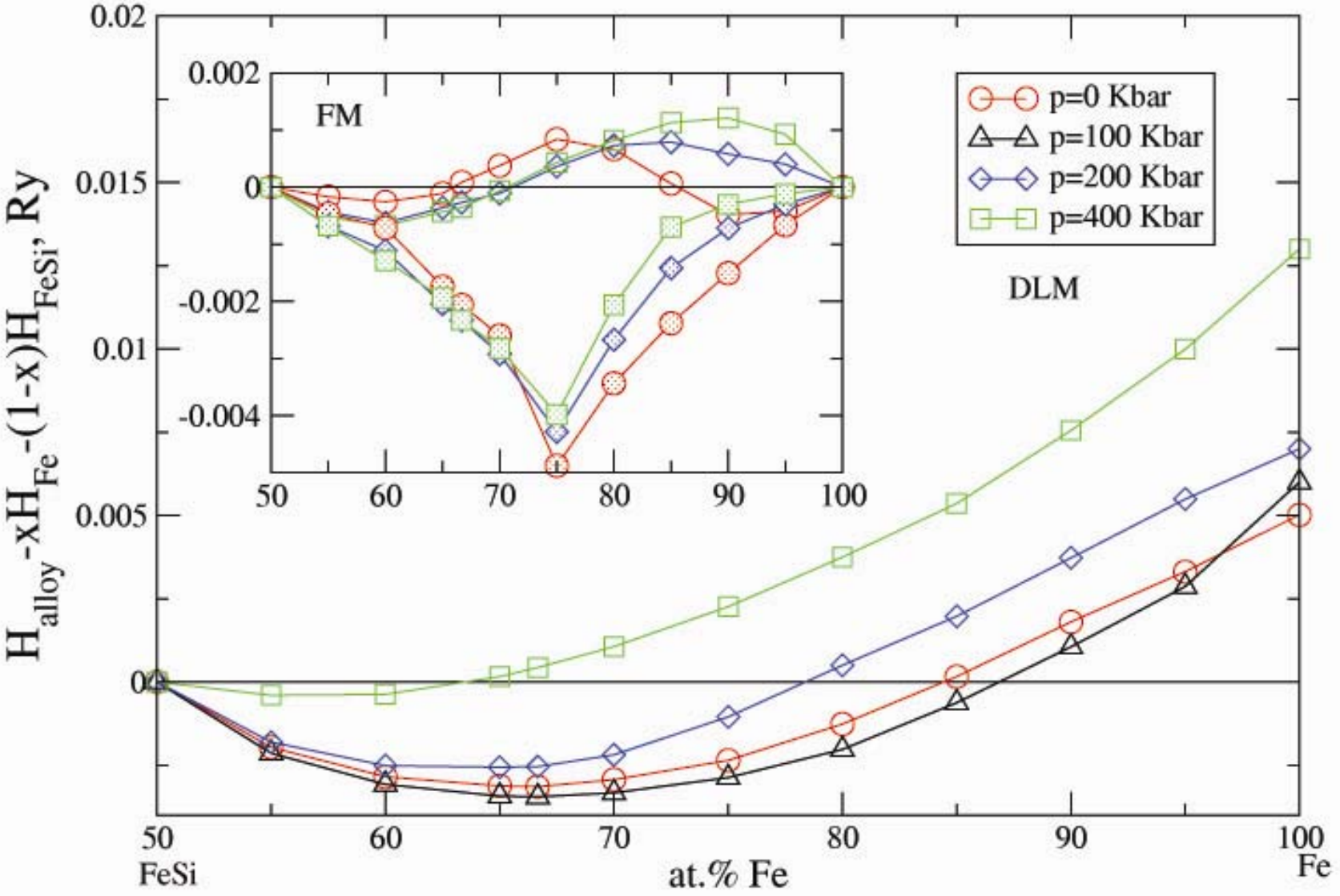
0.02
0.015
0.01
0.005
0
50
60
70
80
90
100
FeSi
Fe
at.% Fe
H_{alloy}-xH_{Fe}-(1-x)H_{FeSi}, Ry
FM
0.002
0
-0.002
-0.004
50
60
70
80
90
100
p=0 Kbar
p=100 Kbar
p=200 Kbar
p=400 Kbar
DLM

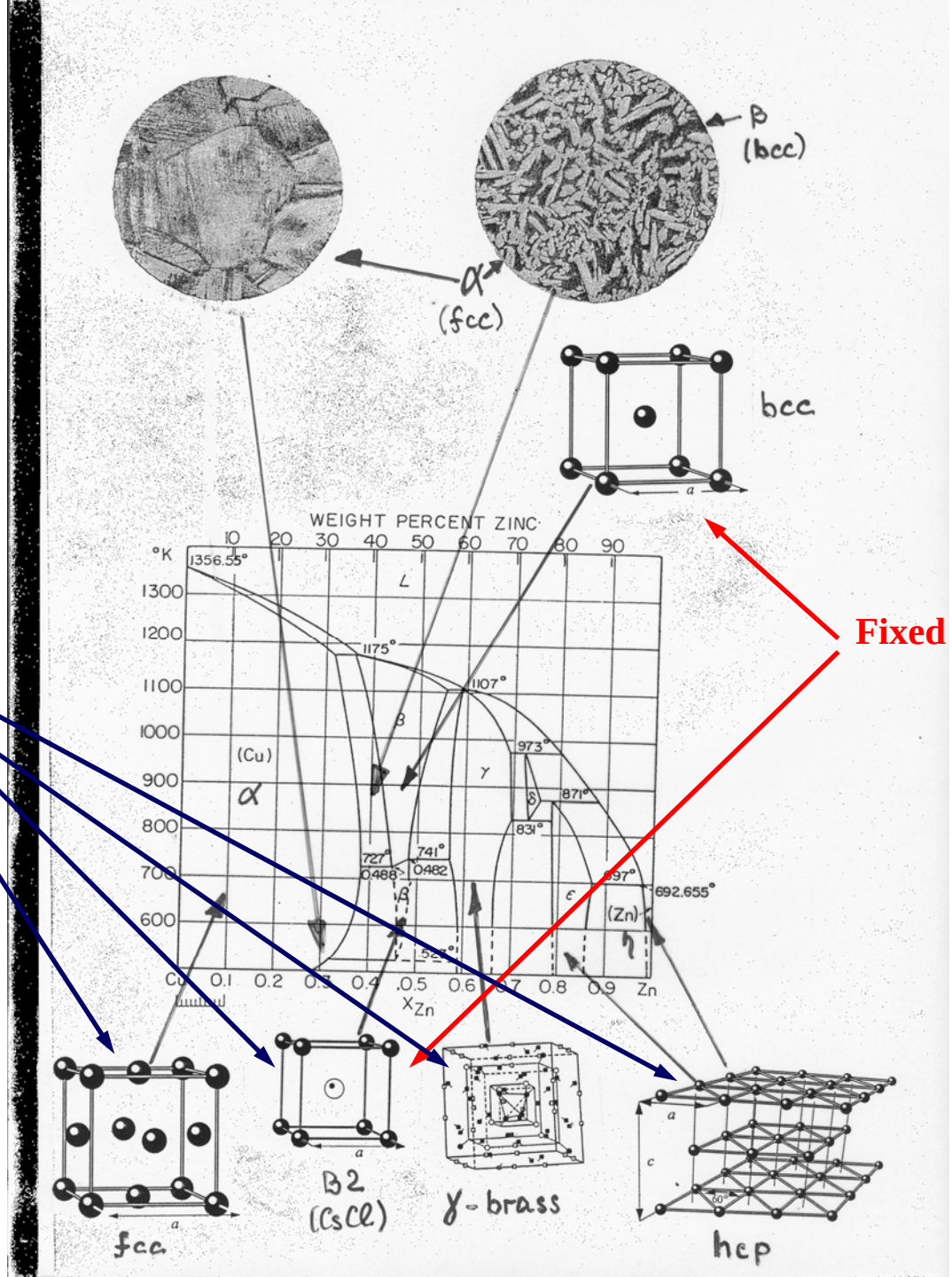

Different underlying lattices

Fixed underlying lattice (bcc)

The Monte Carlo method and the thermodynamic integration

Calculations of averages at temperature *T*:

$$\langle A \rangle = \frac{\sum_s A_s \exp\left(-\frac{E_s}{k_B T}\right)}{Z}$$

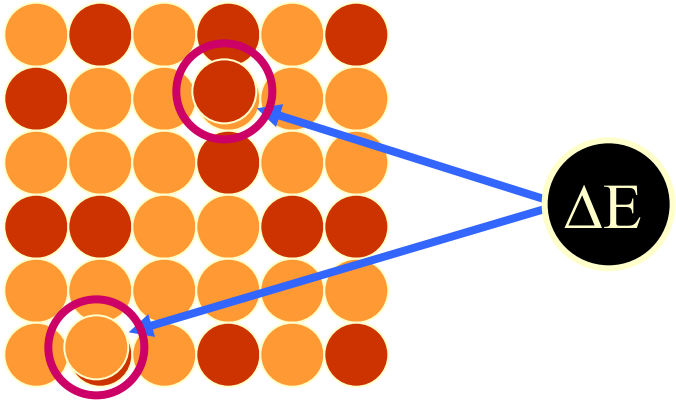

$$\begin{cases} \Delta E \le 0 \\ \Delta E > 0 \quad \exp\left[-\frac{\Delta E}{k_B T}\right] > r \quad (0 \le r \le 1) \end{cases}$$

Atoms exchanged

One can therefore calculate <E>, heat capasity C_V, and use thermodynamics:

$$S(T_2) = S(T_1) + \int_{T_1}^{T_2} \frac{C_P}{T} dT; \qquad C_P = C_V + BVT\alpha^2$$

where B is bulk modulus and α is thermal expansion coefficient

Gibbs-Helmholtz relation:

$$\left(\frac{\partial F/T}{\partial 1/T}\right)_{VT} = E$$

$$S_{conf}(T) = \Delta S_{ideal} + E(T)/T - k_B \int_0^{\beta} E(\beta) d\beta, \qquad \beta = \frac{1}{k_B T}$$

Thermodynamic integration

1) Let $U(\boldsymbol{R}_1, \ldots \boldsymbol{R}_N)$ be the first-principles total energy of the system in which the N nuclei are fixed at positions $\boldsymbol{R}_1, \ldots \boldsymbol{R}_N$.

2). Define continuously variable energy function $U(\lambda)$ such that for $\lambda=0$ $U(0)$ allows one to calculate F easily, and for $\lambda=1$ $U(1)=U$, the potential energy for the system of interest . For instance,

$U_\lambda = (1 - f(\lambda))U_0 + f(\lambda)U$, where $f(\lambda)$ is an arbitrary continuous and differentiable function of λ with the property $f(0)=0$ and $f(1)=1$.

$F_\lambda = -k_B T \ln \left\{ \frac{1}{N!\Lambda^{3N}} \int_V d\mathbf{R}_1 \ldots d\mathbf{R}_N \, e^{-\beta U_\lambda(\mathbf{R}_1, \ldots \mathbf{R}_N; T)} \right\}$, where Λ is the thermal wavelength of the nuclei.

3). Differentiating this with respect to λ gives:

$$\frac{dF_\lambda}{d\lambda} = -k_B T \frac{\frac{1}{N!\Lambda^{3N}} \int_V d\mathbf{R}_1 \ldots d\mathbf{R}_N e^{-\beta U_\lambda(\mathbf{R}_1, \ldots \mathbf{R}_N; T)} \left(-\beta \frac{\partial U_\lambda}{\partial \lambda}\right)}{\frac{1}{N!\Lambda^{3N}} \int_V d\mathbf{R}_1 \ldots d\mathbf{R}_N e^{-\beta U_\lambda(\mathbf{R}_1, \ldots \mathbf{R}_N; T)}} = \left\langle \frac{\partial U_\lambda}{\partial \lambda} \right\rangle_\lambda , \quad \Leftrightarrow$$

$$\Delta F = F - F_0 = \int_0^1 d\lambda \left\langle \frac{\partial U_\lambda}{\partial \lambda} \right\rangle_\lambda .$$

A simple way of defining $U(\lambda)$ is: $U_\lambda = (1 - \lambda) U_0 + \lambda U$. $\Leftrightarrow$

$$\Delta F = \int_0^1 d\lambda \, \langle U - U_0 \rangle_\lambda .$$

METADYNAMICS [A. Laio and M. Parrinello, PNAS **99**, 12562 (2002)]

1). Assume that that there exists a finite (small) number of relevant collective coordinates s_i and considered the dependence of the free energy $F(s)$ on these parameters.

2). The dynamics was defined from the discretized evolution equation: $\sigma_i^{t+1} = \sigma_i^t + \delta\sigma \frac{\phi_i^t}{\left|\phi_i^t\right|}$

where scaled variables are $\sigma_i^t = s_i^t / \Delta s_i$ and $\phi_i^t = (-\partial F(s) / \partial s_i^t)\Delta s_i$ are the scaled forces.

3). Replace the forces with a history dependent term by adding a Gaussian at every point $\sigma^{t'}$ already visited in order to discourage the system to visit it again:

$$\phi_i \rightarrow \phi_i - \frac{\partial}{\partial \sigma_i} W \sum_{t' \le t} \prod_i \exp\left(- \frac{\left|\sigma_i - \sigma_i^{t'}\right|^2}{2\delta\sigma^2} \right)$$

4). The height W and the width δσ of the Gaussian have to be chosen to provide a reasonable compromise between accuracy and efficiency.

5). Explore the free-energy landscape!

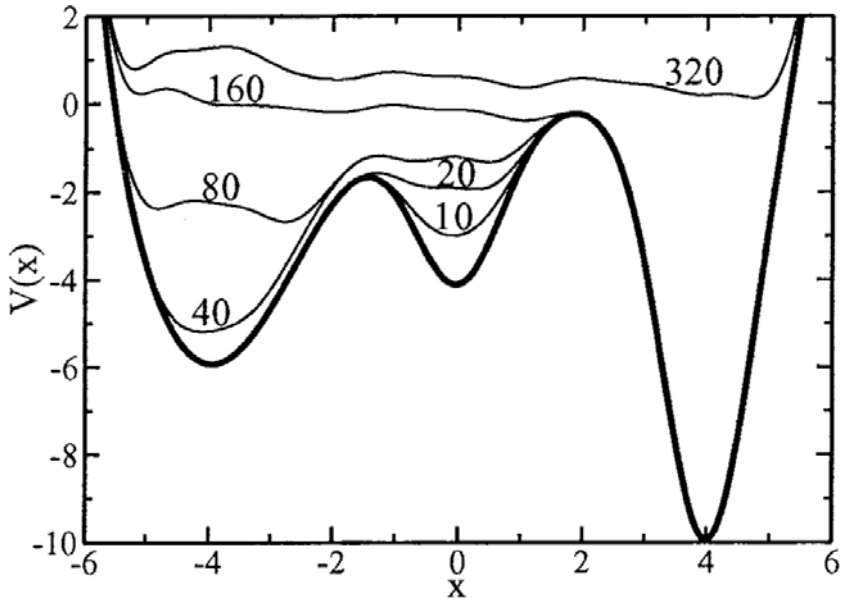

Fig. 1. Time evolution of the sum of a one-dimensional model potential $V(\sigma)$ and the accumulating Gaussian terms of Eq. **2**. The dynamic evolution (thin lines) is labeled by the number of dynamical iterations (Eq. **1**). The starting potential (thick line) has three minima and the dynamics is initiated in the second minimum.

Example: a search for the $MgSiO_3$ post-perovskite phase

(A. R. Oganov *et al.*, Nature **438**, 1142 (2005).

Ab initio simulations based on the GGA and using PAW-VASP

The time step for MD was set to 1 fs.

In *ab initio* calculations 0.7 ps was used for equilibration and 0.3 ps for pressure tensor calculations.

Simulated conditions:150 GPa, 1,500 K.

The supercells used in our calculations contained 160 atoms

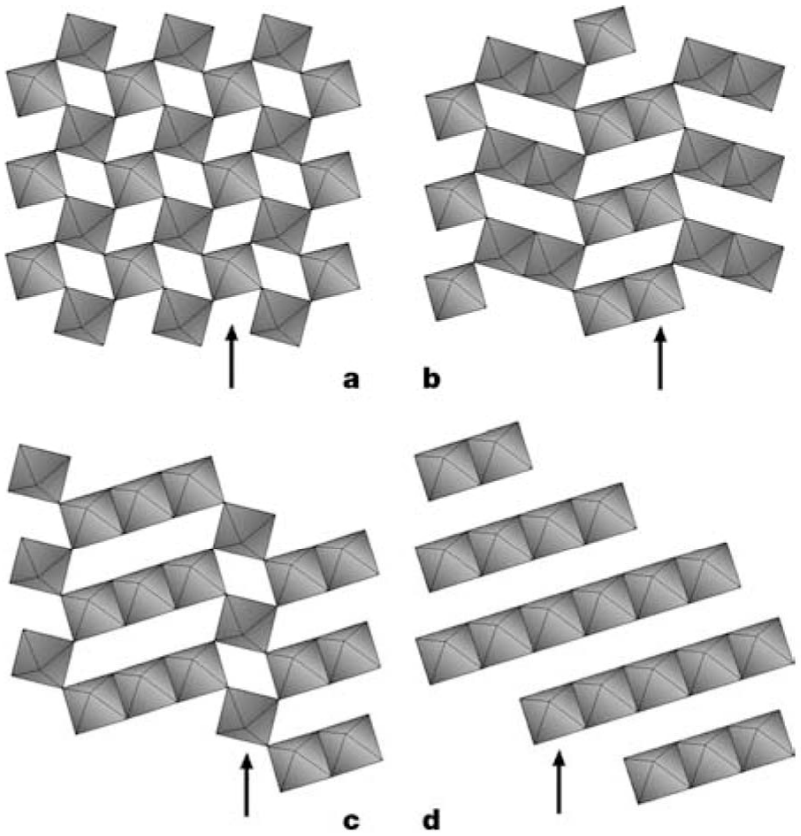

Figure 1 | $MgSiO_3$ polytypes found by metadynamics. **a**, Pv (space group *Pbnm*); **d**, pPv (*Cmcm*); **b**, **c**, newly found structures 2 × 2 (*Pbnm*) and 3 × 1 ($P2_1/m$), respectively. Only silicate octahedra are shown; Mg atoms are omitted for clarity. In the pPv structure, the previously expected slip plane is parallel to the sheets formed by silicate octahedra; the most likely slip plane identified here is shown by an arrow. Arrows also show slip planes in the other structures.

GENETIC OR EVOLUTIONARY ALGORITHM

1). Produce the first population "parents" of structures randomly. Screen off *a priory* impossible structures by using some hard constrains (the minimum acceptable interatomic distances, the minimum value of the lattice parameter, and the minimum and maximum cell angles, etc.). Carry out local optimization of the crystal structures for the "parents". Calculate fittness.

3). Based on the fitness ranking, reject a certain number of the worst structures among the locally optimized ones. The remaining "parents" participate in creating the next generation

4). Create common shapes via similarity transformation: $\mathbf{S_I}=\mathbf{A^{-1}R_I}$, where $\mathbf{S_I}$ are the so-called fractional coordinates, $\mathbf{R_I}$ Cartesian coordinates, and **A** the 3 X 3 matrix of the lattice vectors.

4). Mate in real space using the periodic cuts.

5). Mutations may consist of swaps between different atoms in the cells, as well as of random changes of cell vectors and atomic positions.

6). Screen the "offsprings" by using the same hard constrains as for the "parents", and optimize their structures.

7). The new pool of "parents" is now created.

8). Repeat the whole procedure until some halting criterion is met.

PHYSICAL REVIEW B **73**, 224104 (2006)

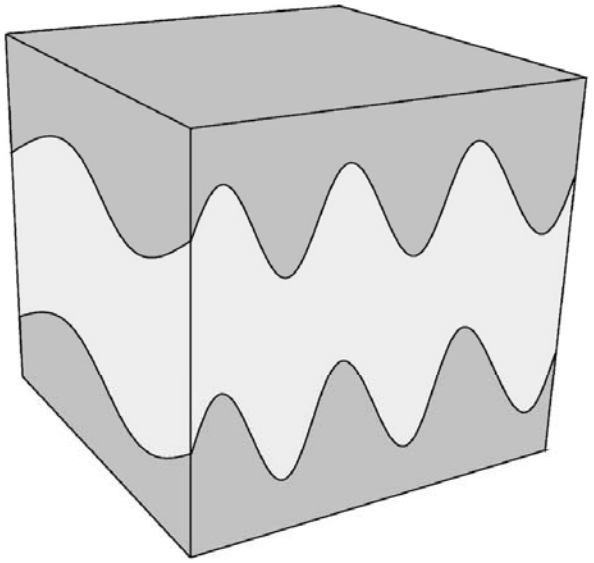

FIG. 2. Real-space representation of the periodic cuts in the crossover operation. Different wavelengths and amplitudes can be used for the cuts along the different cell directions. The cuts are calculated in fractional coordinates which allows crossover between parents with different cells. The dark gray sections represent one part of the cell, the light gray the other, and it is these parts that are swapped in crossover.

Contents:

- Phase stability: general consideration and phenomenological approaches.
- Empirical models (Miedema's empirical model for enthalpies of formation, Pettifor structural map, Hume-Rothery rules).
- Calculations of phase diagrams. Thermodynamic approach.
- From thermodynamics towards statistical mechanics.
- The cluster expansion method
- The Monte-Carlo method
- The global structure optimization problem